CHAPTER

3

Ground-based remote sensing of the shallow subsurface: Geophysical methods for environmental applications

Giorgio Cassiani[a], *Jacopo Boaga*[a], *Ilaria Barone*[a], *Maria Teresa Perri*[a], *Gian Piero Deidda*[b], *Giulio Vignoli*[b], *Claudio Strobbia*[c], *Laura Busato*[d], *Rita Deiana*[e], *Matteo Rossi*[f], *Maria Clementina Caputo*[g], *Lorenzo De Carlo*[g]

[a]Dipartimento di Geoscienze, Università di Padova, Padova, Italy [b]Dipartimento di Ingegneria Civile, Ambientale e Architettura, Università di Cagliari, Cagliari, Italy [c]Realtimeseismic SA, Pau, France [d]Department of Agricultural Sciences, University of Naples Federico II, Naples, Italy [e]Dipartimento di Beni Culturali (dBC), Università di Padova, Padova, Italy [f]Engineering Geology (LTH), Lund University, Lund, Sweden [g]IRSA CNR, Bari, Italy

OUTLINE

1 Introduction

Retrieving information using remote sensing methods is not a new concept when it comes to investigating the shallow subsurface. Noninvasive methods have been developed and used for well over a century, initially for the purpose of mining exploration (e.g., Telford et al., 1990), but with further extension to other application areas. The discipline has been variously called Applied Geophysics, Exploration Geophysics, and Geophysical Prospection. The reason for using the term "geophysics" will be clearer as we discuss the relevant methods.

Recently, as environmental issues have received increasing attention, the shallow subsurface has been the subject of renewed focus for noninvasive methods. The result is that a number of specifically designed methods have been developed for environmental applications. Correspondingly, it is now common to refer to such methods as "Near-Surface Geophysics," or "Environmental Geophysics" and "Hydrogeophysics" because the focus is on environmental and/or hydrological/hydrogeological problems. The development of new terms is partly motivated by an attempt to be more precise, and by the development of a jargon where specialists recognize themselves. Here we will cast all such terms into a common framework, as the ensemble of the relevant methods and applications is, in our opinion, a single discipline that spans many applications.

In the ensuing parts of this chapter, we will first describe the methodologies in their general terms in order to introduce the reader to the nuts and bolts of the methods (Section 2). Some basic understanding of physics are potentially needed here, but to ensure accessibility to a wide range of readers, we avoid equations and try to make the description as understandable as possible, directing readers interested in the details to more specialized sources. Section 3 is devoted to applications, with separate attention to different classes of problems to be solved in this area, and specifically to the issues of defining the system geometry and its fluid dynamics. For the very specialized area of detecting the possible presence and distribution of contaminants in the subsurface, we have only provided relevant references. Section 3 has no ambition to be fully comprehensive: examples are provided solely from the authors' experience, and all material shown here is novel and yet unpublished. Some limited references to the work of the wider community are given. Section 4 covers technological advances and future challenges beyond current techniques.

2 Methods

The general approach of noninvasive geophysical methods can be summarized as shown in Fig. 1. Geophysics is a discipline based purely on physical measurements that are in most cases (but not all) performed at the soil surface, and in all cases at the boundary of a domain of interest. The domain is often the soil below our feet (thus the prefix geo-), but the same methodologies can be applied to other features, for example, to man-made structures such as walls, railways, embankments, and mechanical parts. Such techniques are sometimes called Nondestructive testing or NDT. Noninvasive geophysical methods are conceptually analogous to medical imaging techniques such as X-ray, CT scanning, and magnetic resonance imaging, with the only difference being the physical processes used to obtain images.

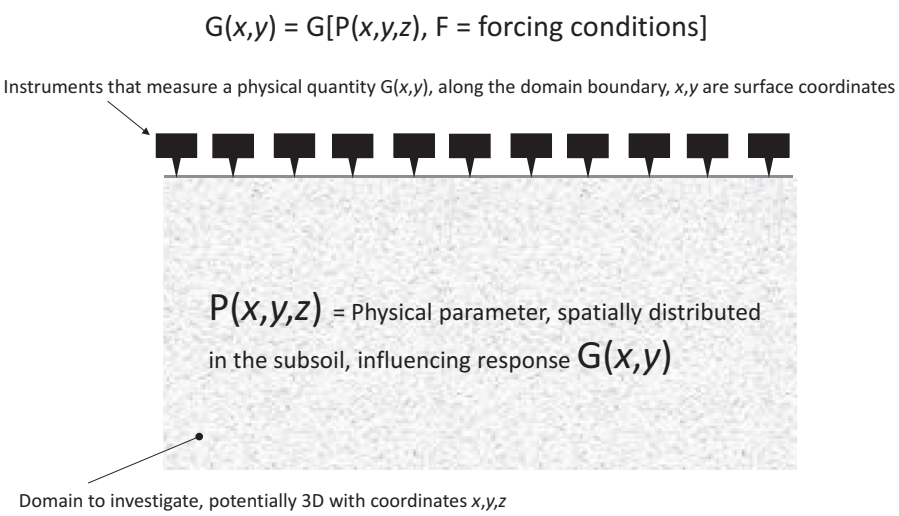

FIG. 1 A general conceptual framework for geophysical measurements.

The general framework can be summarized as follows: a physical instrument collects data concerning a physical quantity G. In general, G is a function of the spatial coordinates along the outer surface, often the ground surface, i.e., G(x, y).

The information content of the function G(x, y) lies in its physical link to a spatially distributed physical parameter P(x, y, z). This parameter depends on soil/rock properties and its state (e.g., water content, temperature). This property is potentially time-dependent so, more generally, we can consider the state variable G(x, y, t)—e.g., soil vibration—and P(x, y, z, t).

P, together with the forcing conditions F that might be required to obtain a measurable signal, is thus responsible for the physical response G. The functional relationship [P,F] → G contains the physics of the phenomenon in question, and is, in general, the solution of a partial differential equation constrained with suitable boundary and initial conditions, where G(x, y, t) is the unknown to be determined (the state variable) and P(x, y, z, t) is the parameter modulating the partial differential equation.

[P,F] → G is generally referred to as the "forward model," i.e., the model that allows the prediction of the system's response, once the system's structure P(x, y, z, t) is known. From a practical standpoint, knowledge of [P,F] → G is essential but still insufficient to characterize the subsurface, as our aim is generally the retrieval of P(x, y, z, t) from G(x, y, t) and not vice versa. A very general schematization of geophysical activities is shown in Fig. 2: while the physics produces a signal G given P, our analysis aim is to retrieve P given the measured G (still accounting for the forcing conditions F). This latter process is named "inversion" and the conceptual inverse function [G,F] → P is named the "inverse model." Before inversion can be conducted, it is, however, necessary that the measured G be cleaned of any "noise" component, i.e., any physical signal that is NOT generated by the system's particular physics, i.e., the particular [P,F] → G we are considering: this step is named signal "processing" (Fig. 2).

The inversion step in Fig. 2 is the essential component of geophysics, and not a trivial one. In fact, no matter which imaging technique we apply, there is no such thing as a closed-form inverse function [G,F] → P. We can only retrieve P(x, y, z, t) by conducting an inversion

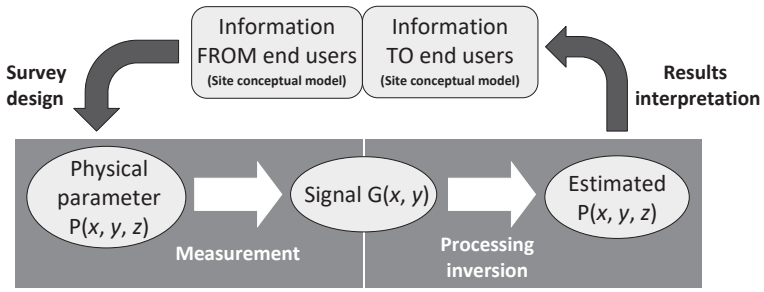

FIG. 2 Measurement and inversion in applied geophysics. Note that this is potentially a virtuous cycle where successive deepening of the investigation may be required.

process that consists in fitting the measured G with the predicted [P,F]→G. This approach is equivalent to calibrating the forward model [P,F]→G onto the field data G, effectively varying the parameter P controlling G.

Such calibration can be performed on any dataset G. Unfortunately, there is no guarantee that a unique solution can be achieved within the error bounds of data from G. The core problem is that multiple spatial and temporal distributions of P(x, y, z, t) may satisfy [P,F]→G on a given dataset, that is, solutions are not unique. Thus, in designing geophysical surveys the key goal of the practitioner is to implement a design that results in a solution of the inverse problem that is as unique as possible in the region of interest. This involves a full understanding of the practical problem to be solved: the relationship with the end user must be close, and the flow of information must go both ways. Of course, the results of geophysical surveys must be communicated to the end user in order to facilitate a valid (possibly joint) interpretation (Fig. 2). A solid understanding of the final user's needs is critical for the geophysicist in order to design the survey. Fig. 2 also shows a link from the a priori knowledge of the end user to the geophysical survey design. On the basis of this a priori information, the geophysical survey shall be planned in order for the nonuniqueness of geophysical inversion to have minimal or no impact on the region of interest and, crucially, on the problem of interest. The final goal is always to develop a conceptual model of the site that is consistent with all available data, including the newly acquired geophysical data. All conceptual models of the site that satisfy the measured geophysical data may in fact have features in common and other alternative conceptual models (that may have been plausible at the start) may be ruled out as their geophysical response would not be consistent with the observed data.

It is not uncommon that multiple forms of integrated geophysical data are collected at the same site. In this case, while each individual data inversion may lead to some nonunique results, the joint consideration of the two sets of plausible inverted models may lead to the identification of one or more conceptual models that satisfy all the available data (including non-geophysical data). This type of joint data analysis, and sometimes joint data inversion, can be extremely powerful but at the same time requires extra care in order to consider all data with respect to their actual information content, resolution, and reliability.

TABLE 1 Methods, measured quantities, physical parameters, and forcing conditions

Method	G	P	F
DC (direct current) electrical resistivity methods (often called geo-electrical methods—and in particular, electrical resistivity tomography—ERT)	Voltage	Electrical resistivity	Current intensity
Seismics	Soil vibration	Seismic velocity/impedance	Mechanical source
Ground penetrating radar (GPR)	Electrical field	Dielectric constant (velocity/impedance)	Electrical pulse
Geo-magnetism	Magnetic field	Magnetic susceptibility/permanent magnetization	None
Gravity	Gravitational acceleration	Density	None
Electromagnetic induction (EMI)	Secondary (time-varying) magnetic field	Electrical conductivity (1/resistivity)	Inducing magnetic field
Induced polarization (IP)	(Time-varying) Voltage	Chargeability	(Time varying) current intensity
Spontaneous potential (SP)	Voltage	Electrical resistivity	Natural current sources

All geophysical methods can be cast in the general framework described above. Of course, large differences may arise because of the different nature of the physical relationship $[P,F] \rightarrow G$ that lies at the heart of the method. More specifically, the physical definitions listed in Table 1 apply.

Each geophysical method leads to imaging the subsurface in terms of at least one (and usually, but not always, only one) physical parameter P. The information content of the data therefore lies in the values and spatial (sometimes temporal too) distribution of $P(x, y, z, t)$. How this information can be useful for the final user depends on two key aspects of P:

(a) The values of P must be informative in that they represent, albeit indirectly, a variable of direct interest for the problem at hand. Consider, for example, seismic velocity as a proxy for soil mechanical properties or electrical conductivity as indication proxy for pore water salinity.

(b) The spatial distribution of P is informative, albeit not as a direct measure of physical properties, because its different values are indicative of different geological or subsurface formations, or different states of the same formation, so that the "image" of $P(x, y, z, t)$ can be read as an "image" of the subsoil structure (or other features).

One must keep these two possible uses in mind when geophysical methods are chosen and applied to a particular problem. In more specific terms, the following criteria are should always be considered when a selection is to be made between different possible geophysical methods potentially applicable to a real-life application:

(1) The parameter P of the selected geophysical method has to be informative for the goal of specific application, in terms of either (a) physical significance or (b) spatial distribution of the subsurface.

(2) Once (1) is satisfied, the selected method has to have sufficient penetration to reach the required depth of investigation, and sufficient resolution to highlight the desired features at that depth. This requirement depends on, of course, both the physics of the problem ([P,F]$\rightarrow$G) and the survey design (including accessibility to a larger or smaller area of the bounding outer surface). In some cases, an appropriate survey design is sufficient to meet such a requirement (e.g., often for electrical resistivity tomography (ERT)), while in other cases the physics dictates the limit (e.g., for ground penetrating radar (GPR) and electromagnetic induction (EMI)).

Criteria (1) and (2) must be passed by any geophysical method to be considered useful for the practical goal ad hand. Once these criteria are satisfied, a number of other factors should be taken into account for further selection among the suitable methods: cost, logistics, and environmental impacts. However, these further requirements have no impact on the choice of method if the first two requirements are not met.

Shallow geophysical investigations, such as those focused on geomorphological issues, must take into account three key aspects of the subsurface (Fig. 3):

- structure
- (fluid)dynamics
- contamination (at contaminated sites)

Different geophysical methods have different sensitivities to the three subsoil components as shown in Fig. 3. While a general classification is hard to draw, Table 2 presents some indications on the relative suitability of the most common geophysical techniques for highlighting structure, dynamics, and contamination in the shallow subsoil.

When applying geophysics to a site of geomorphological interest, and thus to relatively shallow depths (tens of meters at most), one should always keep in mind that structure, fluid dynamics, and (when applicable) contamination all affect the geophysical signal G.

While this can be seen as a disadvantage if we are interested only in one component of the problem (e.g., structure), this fact can also be an advantage in that all components can be potentially extracted from geophysical data, provided that the individual effects on the geophysical signal are separated. For this process to fully achieve its goals, it is often necessary to couple geophysical measurements with a mechanistic model that can incorporate structure and on this basis predict dynamics and possibly also contaminant distribution. This model can therefore be calibrated against geophysical and other data, in most cases in their time-lapse changes, thus representing the site's static and dynamic behavior to the best of the available information.

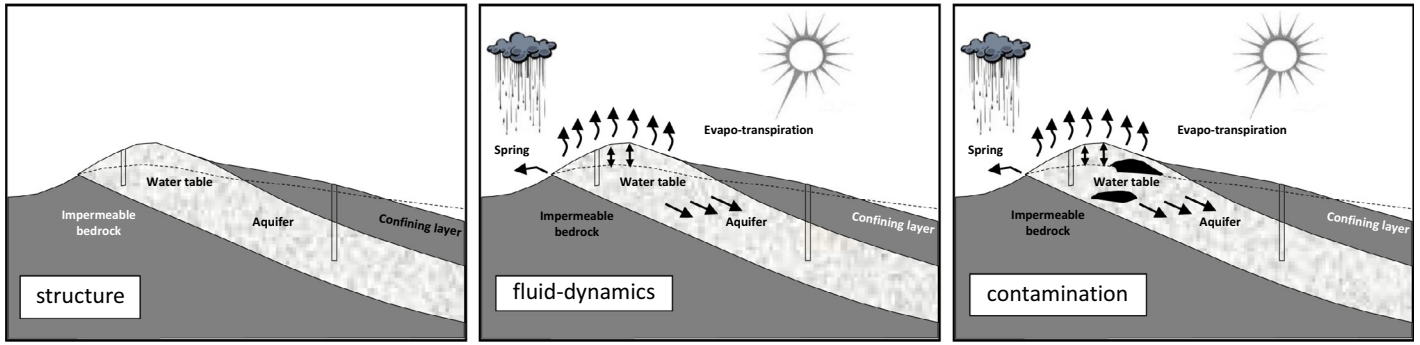

FIG. 3 Aspects of subsoil affecting shallow geophysical investigations.

TABLE 2 Applicable methods and subsurface characteristics: more crosses indicate better applicability

Method	Structure	Dynamics	Contamination
Seismics	+++		
EM methods	++	++	+
DC resistivity methods	++	++	+
Ground penetrating radar	+++	++	+
Magnetics	++		+
Gravimetry	++	++	
Induced polarization	+	+	++
Self-potential		++	++
Nuclear magnetic resonance	+	++	

The indication is purely qualitative. Note that in order to identify (fluid dynamics), time-lapse measurements must be conducted (with the sole exception of self-potential method).

In the following section, we sketch the specific physical and acquisition characteristics of the most common geophysical methods useful in geomorphology. Two very good reviews of methods for near-surface geophysics, and hydrogeophysics in particular (but the reviews are not limited to this topic), can be found in the books by Rubin and Hubbard (2005) and Vereecken et al. (2006).

2.1 Geo-electrical (DC resistivity) methods

The development of methods based on the injection of DC electrical current in the ground, and the measurement of corresponding voltage differences between two electrodes, dates back nearly a century; for classical reviews see, for example, Keller and Frischknecht (1966) and Kelly (1977). The use of Ohm's law allows, under simplifying conditions, the reconstruction of electrical resistivity and the distribution in the subsurface: the original method only provided one-dimensional (1D) vertical soil profiles (vertical electrical soundings or VES) or lateral resistivity 1D profiles. A major step forward was made in the early 1990s with the development of ERT that provides estimates of the spatial distribution [in two dimension (2D) or three dimension (3D)] of electrical resistivity. It can also give insight into the time evolution of electrical resistivity if repeated measurements are used. A comprehensive review of the method, including the use of time-lapse measurements, is given by Binley and Kemna (2005).

ERT is probably the most widely used methodology for near-surface noninvasive characterization as:

(a) it is easy to deploy on the ground;
(b) there is a wide availability of software for data inversion, much of it free and open source;
(c) it requires apparently little technical skill: standard acquisition sequences are often available for standard geometries, and acquisition and inversion can be performed even by untrained personnel;

(d) the spatial variability of electrical resistivity often reflects lithological contrasts as well as of the presence of water and its saline content (consider, e.g., Archie, 1942; Brovelli et al., 2005; Brovelli and Cassiani, 2010). Thus both structure and hydrological dynamics are amenable to be tackled using ERT.

While the advantages of ERT are undeniable, we must stress here how the apparent ease of use of ERT is often deceiving. ERT surveys must be planned carefully, be custom-made and data quality must be checked in detail in order to remove data outliers. In addition, the method requires a firm estimate of data errors in order to control inversion. A good procedure is suggested by Binley et al. (1995) and consists in measuring the resistance of the so-called reciprocal configurations (swapping current with potential electrodes): differences between the two configurations are a good estimate of measurement errors.

We also underline some limitations of ERT. In particular, the highest sensitivity of the method is close to the electrodes. This limits the distance of reliable investigation. In the most common case of surface investigations (i.e., with all electrodes placed at the soil surface), the reliable depth of investigation can be estimated to be about 1/4–1/5 of the electrode line length. Therefore, going to depths larger than 200 m requires electrode lines longer than 1 km, with serious logistic limitations, especially in urban or industrial environments. For deeper electrical investigations, it is common practice to resort to electromagnetic methods (see next section). Similarly, cross-hole ERT investigations require that the two (at least) boreholes equipped with electrodes be placed at a reciprocal distance smaller than their depth.

ERT has been applied successfully to image the shallow subsurface for over 25 years. This includes surface applications, which are the most common, borehole applications (e.g., Bevc and Morrison, 1991), and laboratory investigations (Binley et al., 1996). Another key advantage of ERT is that it does not possess a spatial scale per se: unlike other methods, the resolution depends solely on electrode spacing which can go from centimeters to tens of meters. In addition, time-lapse ERT measurements allow for the imaging of time-varying processes in the shallow subsurface, with obvious links to hydrological processes. Pioneering work was conducted in the 1990s in the United States and the United Kingdom (Daily et al., 1992; Daily et al., 1995; Daily and Ramirez, 1995; LaBrecque et al., 1996; Slater et al., 1997); see Daily et al. (2004) for a review.

We cannot cover the entirety of the scientific literature on ERT here, and so we refer readers to a few exemplar applications concerning contaminated sites (Cassiani et al., 2006), hyporheic zone (Crook et al., 2008), hillslope processes (Cassiani et al., 2009a, 2009b), transport in shallow aquifers (Kemna et al., 2002; Monego et al., 2010; Perri et al., 2012; Singha and Gorelick, 2005; Slater et al., 2000), and monitoring processes in hypersaline environments (Haaken et al., 2017). Some specific examples are given in Section 3.

As a side note, we consider two other geo-electrical methods that differ from ERT and its antecedents in two ways—note that both methods date back to the pioneering work of early 1900s (Schlumberger, 1920):

– The Mise-à-la-masse method (MALM)

MALM is a method originally developed to delineate electrically conductive ore bodies. An electrical current is passed through the body, while the resulting voltage values are

measured at the ground surface or in boreholes. The pattern of the resulting equipotential contour lines gives information on the geometry (shape, extent, dip, continuity) of the electrically conductive body. The same approach can be used for saline tracer tests. In this case, electrical current is injected into the conductive plume and its evolution is monitored with time. Recent applications to landfills and tracer tests can be found, e.g., in De Carlo et al. (2013) and Perri et al. (2018). In general, one can view MALM as a geo-electrical method in which inversion is not attempted in most cases because the geometry of the acquisition or size of the surveyed area do not allow for a sufficient data set to be acquired to image the volume of interest. Nevertheless, the information content of the data may be explored, often using some forward model and the predicted and measured voltage values are compared in a semiquantitative manner.

– The Induced Polarization (IP) method

IP method is a well-established geophysical exploration method (Sumner, 1976). Information concerning the subsoil are inferred from the measured voltage signals associated with polarization currents in the earth caused by a sudden change (switch off or on) in an injected current (hence the term "induced"). The method had already been adopted in the 1960s for the exploration of porphyry and massive sulfides. Acquiring time-domain IP measurements is simple using modern ERT equipment, and can be made at the same time as resistivity measurements. Inversion with imaging is also possible using the chargeability formulation of Seigel (1959). With the advancement of instrumentation, the spectral nature of the IP response, i.e., its dependence on frequency (Spectral-induced polarization or SIP), has been increasingly investigated, with the relevant inversion formulation in terms of complex electrical resistivity (e.g., Kemna et al., 2000).

While IP, particularly in time domain, is often used to image the subsurface, its physical meaning is still elusive. While many mechanisms are known to exist, the relative importance of each is difficult to ascertain in practical applications (in spite of many overambitious attempts) and strong research needs are still unanswered (see Kemna et al., 2012, for a review).

2.2 EMI methods and GPR

Two different classes of exploration methods are based on a more general exploitation of Maxwell's equations of electromagnetism. In particular, once the electrical field is not stationary or quasi-stationary (DC methods), the entire realm of electromagnetic (EM) phenomena are called into play. From this broad spectrum of possible EM responses, two main phenomena may be considered under the umbrella of EMI and GPR:

1. A time-varying magnetic field generates an electrical field (and current, if conductors are present) according to Faraday's law of EM induction.
2. The magnetic field is generated either by an electrical current, which can be described by Ampere's or Biot-Savart's law, or by a time-varying electrical field, which is called a displacement current and was introduced first by James C. Maxwell.

In presence of an electrical conductor (e.g., the soil or the subsoil), the relative importance of the first phenomenon with respect to the second is controlled by the so-called loss factor, i.e., the ratio of electrical conductivity over the product of electrical permittivity and frequency,

which is used for exploration. If the loss factor is larger than one, then EM induction prevails, with diffusion characteristics. In this case EMI methods are possible. If the loss factor is smaller than one, then the entire suite of Maxwell's equations applies, and the EM field behaves like a wavefield that is attenuated as an effect of electrical conductivity. This situation allows the use of what is called GPR.

In a nutshell:

- EMI methods measure electrical conductivity, i.e., the same as DC conductivity methods (electrical conductivity is the reciprocal of electrical resistivity), and they can be used practically in all conditions. However, the propagation of the EM field is diffusive in nature and thus poorly focused. This means that reconstruction (i.e., inversion of data) of the conductivity field is inevitably smeared.
- GPR is a wave propagation method, thus it is based on reflection, refraction, waveguides, travel times, etc. It can exploit principles of geometrical optics, thus inversion is straightforward, even in tomographic terms. However, GPR does not always work. If the investigated medium is too conductive, the signal is destroyed because EM energy is converted to heat via Ohm's law. In that event no investigation is possible. Note that in very resistive environments (such as glaciers) GPR can penetrate hundreds or thousands of meters.

Near-surface applications are common for both classes of methods. Note that EMI includes a very large number of different methods (see, e.g., Telford et al., 1990), that go from very deep (e.g., Magneto-Tellurics) to very shallow (frequency-domain or FDEM) methods. For near-surface investigations, it is common to proceed with FDEM methods that are often carried out using a single coil spacing and a single frequency. In this classical approach it is only possible to produce maps of apparent electrical conductivity—i.e., at each location a single value of electrical conductivity is estimated assuming that the investigated volume is homogeneous. This can yield results both in terms of zonation and of time-lapse changes (e.g., Robinson et al., 2009; Cassiani et al., 2012). Note that EMI investigations of this type are also very useful as preliminary investigations for buried man-made structures (see, e.g., Cassiani et al., 2014). More advanced approaches, involving FDEM inversion and thus depth imaging, will be discussed below.

An alternative to FDEM is given by time-domain EM (TDEM) methods, where the EM induction is triggered by a sudden cessation of current in a loop. This produces eddy currents in the subsoil that propagate similar to smoke rings to deeper regions, while getting larger and larger, and thus losing resolution. Nevertheless, it is still possible to invert the induced secondary magnetic field (generated by Ampere's law) and produce 1D vertical profiles of electrical conductivity. The scale can go from a few meters to hundreds of meters (Nabighian and Macnae, 1991; Christiansen et al., 2006; Auken et al., 2015).

Note that many other EM methods are available. The most notable one is Controlled Source Audio Magneto-Tellurics (CSAMT—Zonge and Hughes, 1991). In all cases, however, the general advantages and limitations of EMI methods apply as described above.

GPR is a classical near-surface method (with the sole exception of glacier exploration, see, e.g., Parsekian et al., 2016). For a comprehensive introduction about GPR see, e.g., Annan (2005).

The applications of GPR to near-surface problems are manifold. Three aspects shall be considered:

- GPR is a wave-propagation method: therefore, it is capable of "seeing" contrasts in reflection coefficients as determined primarily by electrical permittivity contrasts. Thus, it is a very effective method to characterize the structure of the near surface. This characterization can extend tentatively, down to 10 wavelengths under normal electrical conductivity values, i.e., under attenuation conditions. In practice, however, the deepest imaging depth is at most 10–20 m from the ground surface, excluding imaging through ice. A nice example is given, e.g., by Klenk et al. (2015) where the dependence of the images on changing GPR velocity is also shown as a function of changing soil moisture content. The influence of soil moisture is discussed in the following.
- The velocity of the GPR EM wave depends, under normal conditions, solely on the electrical permittivity of the medium. This in turn depends, in the case of natural porous media, predominantly on the volumetric moisture content. Classical relationships have been established long ago (e.g., Topp et al., 1980); for a review see Klotzsche et al. (2018). Thus repeated GPR measurements can provide quantitative estimates of changing moisture content. This is irrespective of possible changes in soil water salinity that alter electrical conductivity in the same way as changing moisture content (a limitation for DC electrical methods such as ERT). However, GPR resolution depends on wavelength that in turn depends on source frequency. Tentatively, a typical frequency for geological investigation is 100 MHz, which corresponds to a wavelength of about 1 m. The highest frequencies (say 1 GHz) correspond to about 10 cm wavelength, with the corresponding penetration limited to about 1 m—there is no such thing as a free meal!
- Because GPR energy is attenuated as a function of the electrical conductivity of the conducting medium, it is possible to estimate conductivity from attenuation. Some attempts have been made (e.g., Day-Lewis et al., 2003), even though amplitudes of GPR signals are also affected by source directivity and geometric spreading. In addition, ERT is surely a much simpler approach to measure electrical conductivity.

Not surprisingly, GPR has proven very popular in near-surface applications. GPR can be used both at the surface and in boreholes. Leaving aside the simplest surface measurements for structure characterization (see an example in Section 3), GPR has been used for:

- time-lapse GPR data collection from the surface to image infiltration processes (e.g., Van Overmeeren et al., 1997);
- surface measurements affected by complex propagation modes in waveguides that are nevertheless very informative (Arcone, 1984; Arcone et al., 2003; Strobbia and Cassiani, 2007);
- surface applications to estimate soil moisture content in agricultural contexts (e.g., Grote et al., 2003; Huisman et al., 2003);
- cross-hole and hole to surface applications aimed at viewing structure and hydrological dynamics in the subsurface, sometimes in conjunction with ERT monitoring

(Alumbaugh et al., 2002; Hubbard et al., 1997; Binley et al., 2002a, 2002b; Binley and Beven, 2003; Cassiani et al., 2004, 2008; Schmalholz et al., 2004; Cassiani and Binley, 2005; Deiana et al., 2007, 2008; Looms et al., 2008);
- advanced inversion approaches to fully exploit the information content in GPR propagation (e.g., Keskinen et al., 2017).

2.3 Seismics

The propagation of elastic waves in the subsurface is the basis of the most widely used geophysical exploration methods (Yilmaz, 2001). Being a wave-based method, seismic methods are focused and well amenable to imaging. Yet, for the near-surface applications as considered herein, seismic methods are often *not* the method of choice. The main limitation lies in the typical wavelengths of seismic wave that are often, with high frequencies, at least in the range of tens of meters. Although in some cases a combination of high frequencies and S-wave propagation may help in achieving high resolution (e.g., Deidda and Balia, 2001; Petronio et al., 2016); in general the classical seismic reflection method is unsuitable for shallow applications. Seismic refraction is an alternative approach based on Snell's law and tracking of rays from sources to receivers (e.g., Zhang et al., 1998), and is widely applied in near-surface investigations. However, the most promising approach is probably the use of surface waves, and Rayleigh waves in particular (Aki and Richards, 2002). These waves are the solid equivalent of the waves on the surface of a fluid. Early attempts to extract information from surface waves date back to Jones (1958, 1962). A major step forward was made in the 1980s with the Spectral Analysis of Surface Waves developed by Nazarian and Stokoe II (1984) and with the historical progress in electronics and computers, which made it possible to devise multichannel techniques or Multichannel Analysis of Surface Waves (McMechan and Yedlin, 1981; Park et al., 1999).

The information carried by Rayleigh waves lies in their dispersive characteristics: different frequencies travel at different speeds, and different frequencies involve different thicknesses below the ground surface, with lower frequencies involving deeper portions of the subsurface. The classical approaches produce 1D vertical profiles of shear wave velocities, the parameter that chiefly controls Rayleigh wave propagation. New techniques are being devised to produce laterally varying images of the shear wave velocities. For a complete overview, see the book by Foti et al. (2017).

3 Application examples

The number of specific applications of near-surface noninvasive techniques is very large, ranging from geomorphological studies to the characterization of contaminated sites, from hydrogeological/hydrological problems to geotechnical characterization. In this section, we presented illustrative examples stemmed from our own experience. In particular, we list examples that are mainly focused on the structural characterization of the subsurface and others where the main interest is the fluid dynamics in the subsurface.

3.1 System structure

3.1.1 The Settolo site

This site lies on the left bank of the Piave River, close to the city of Valdobbiadene, NE Italy. For a complete site description, see, e.g., Perri et al. (2012). The site is on a riparian aquifer used for irrigation and drinking water supply. As the water table is at an average depth of about 5–6 m b.g.l., with seasonal oscillations depending on the Piave River stage, the aquifer is very vulnerable to contamination from the surface. The area is made of alluvial sediments of the Piave River composed of gravel in a sandy matrix. With the exception of a conglomeratic moraine terrace probably of fluvio-glacial origin that stands about 40 m above the neighboring alluvial plain in the northern side of the site, the study area has no particular geomorphologic characteristics. The moraine that emerges on the sides of the alluvial plain also underlies the fluvial gravel, and forms its hydrological bedrock. The riparian aquifer geometry is relatively complex due to the presence of several buried paleo-river channels, filled with the gravelly sandy sediments. These paleo-channels are easily detectable by large-scale surface ERT surveys.

Fig. 4 shows an instructive example of data taken along the same line across the main deposition and flow direction, showing the ERT results obtained using two different ERT

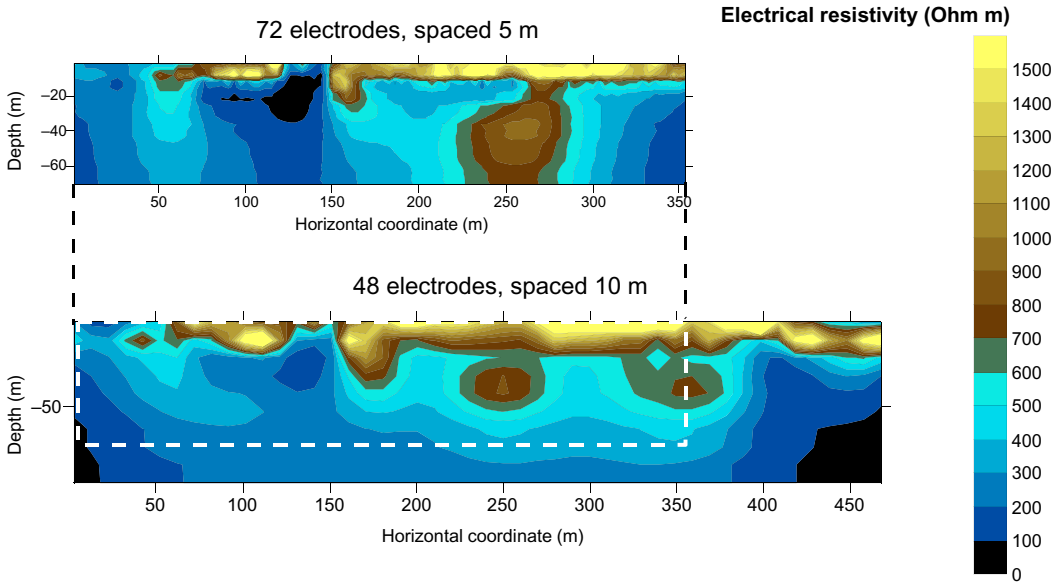

LINEA 2
La Linea 2 (indicata in giallo in fig. 3) è stata acquisita procedendo da NE a SO con 48 elettrodi equispaziati 10 m per un totale di 470 m.
Al fine di valutare la qualità del dato aumentando la risoluzione, cioè riducendo a spaziatura interelettrodica e portandosi a profondità di investigazione ridotte, rispetto a quelle ottenute con la spaziatura 10 m, sulla stessa linea è stata acquisita una tomografia con 72 elettrodi e spaziatura interelettrodica pari a 5 m, per un totale di 355 m di sviluppo lineare ed una profondità di investigazione di poco più di 60 m rispetto al piano campagna. I risultati dell'inversione per la Linea 2, con le due differenti spaziature, sono riportati in fig. 6.

FIG. 4 Settolo site: ERT lines along the same profile. See discussion in the text.

configurations: a higher resolution setup, using 72 electrodes spaced at 5 m, and a lower resolution setup using only 48 electrodes spaced at 10 m. Both these setups provide subsurface information, but the spacing of the latter, although leading to lower resolution information, allows deeper penetration of the subsurface. In both cases, a classical Wenner-Schlumberger configuration was used, offering a good balance between resolution and penetration. The instrument used was an Iris Instruments Syscal Pro resistivity meter. The inversion was performed using the Occam's inversion freeware profiler/R2t by A. Binley (www.es.lancs.ac.uk/people/amb/Freeware).

A comparison between the two ERT lines demonstrates some of the method's characteristics. Both images show comparable anomalies: in both cases the deeper moraine is more electrically conductive than the gravel in the channels, and the contrast is large enough to provide a clear geometric image of the two formations. However, the shorter, high-resolution line shows deeper anomalies as more vertically extensive—consider, e.g., the gravel body at about 250 m in the section. The same body is clearly delineated in the longer, lower resolution line, as current lines go deep enough so as to go around this resistive body and carry to the surface the relevant information (in terms of voltage differences). The shorter line also fails to detect the resistive body at 350 m that is apparent in the longer line because this anomaly is located at the right extreme of the short section, there are very few current lines crossing that area, and all of them are consequently collecting information on a much larger volume.

In general, near the ends of the surveys and at depth, ERT imaging capabilities are diminished. On the other hand, a smaller electrode spacing has also clear advantages in terms of resolution, in the region where imaging is accurate. The water table appears much sharper in the shorter line than in the longer line, at a depth between 5 and 10 m (i.e., between 1 and 2 electrode spacings—note that is it probably around 6 m). Also, the shallow conductive anomaly at 130 m—a gas pipeline—is much more sharply seen by the line at 5 m spacing than by the other.

3.1.2 The Trecate site

The contaminated site near Trecate (Novara, NW Italy) is the result of a dramatic incident: in 1994, a crude oil blowout took place from the TR24 well undergoing side-track drilling. Approximately 15,000 m^3 of middle weight crude oil were released overland, contaminating both soil and groundwater. For a thorough discussion of the site and the state of its contamination, see, e.g., Burbery et al. (2004) and Cassiani et al. (2014). The site is characterized by a thick sequence of poorly sorted silty sands and gravels in extensive lenses, typical of braided river sediments. An artificial layer of clayey-silty material, about 1–2 m thick, placed as a liner for rice paddies, overlies most of the site. Fig. 5 shows the results of one GPR line conducted at the site using a PulseEkko Pro system with 100 MHz antennas. The survey is a typical zero-offset profile, i.e., transmitter and receiver antennas are placed next to each other and pulled together along the line.

Conversion from two-way time reflection to depth is possible thanks to ancillary data collected using multiple offset GPR configurations: in particular, common depth point as described extensively also in the seismic literature. Fig. 5 shows how the GPR signal penetrates to about 7 m depth, despite the presence of fine sediments (these are potentially electrically conductive) that make the bed of the artificial rice paddies. In particular, the

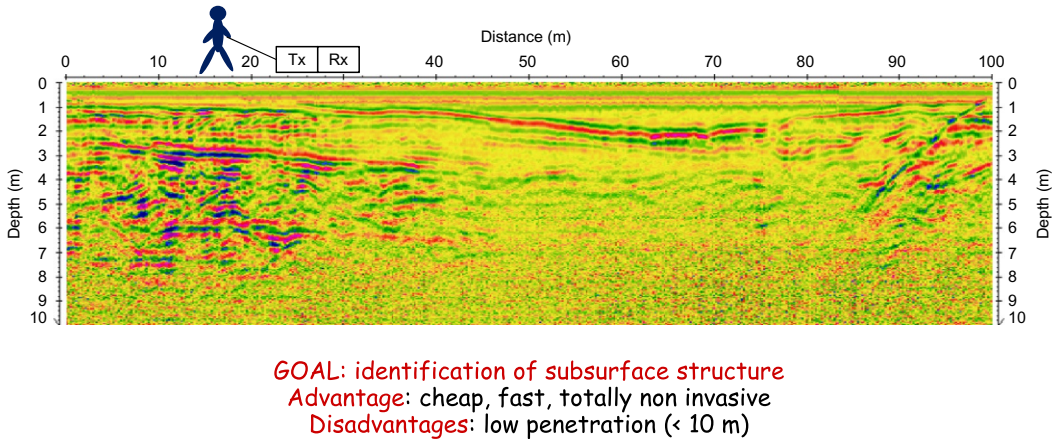

FIG. 5 Trecate site: a 100-MHz GPR line shows the presence of a paleo-channel created by a braided river system. See discussion in the text.

GPR line shows a paleo-channel created by a braided river system, filled with fine sediments, more electrically conductive than the surrounding gravels. The result of this geometry is that the GPR signal is more attenuated below the paleo-channel.

3.1.3 The Aviano site

The industrial area in Aviano, NE Italy, has been the site of major Trichloroethilene/Tetrachloroethilene (TCE/PCE) subsoil contamination that took place before the mid-1980s. The chlorinated solvents have been detected in the deep phreatic aquifer some 12 km downstream of the site, where the water table emerges to the ground surface in a line of springs. Below the site, the phreatic surface is about 100 m deep. Thus, the migration of contaminants took place in the unsaturated zone. More specifically, the site is underlain by a thin silty clay layer (about 1 m thick), at an average depth of about 7 m below ground, that holds above a shallow perched water body. The clay layer is however not continuous everywhere, having been eroded by some paleo-channels that are encountered locally by the monitoring boreholes. These discontinuities allowed infiltration of the contaminated waters toward the deeper continuous phreatic aquifer. Therefore, the detection of these holes in the clay layers is a key aspect of site characterization and remediation. Fig. 6 shows how the clay layer can be easily detected using surface ERT lines. In both cases we used 120 electrodes spaced at 0.8 m, with a dipole–dipole skip 8 configuration (i.e., the current and potential dipoles are 8 m long) and a full reciprocal acquisition. The inversion was performed using the Occam's inversion freeware profiler/R2t by A. Binley (www.es.lancs.ac.uk/people/amb/Freeware).

We note here that the presence of a continuous electrically conductive clay layer (ERT4 in Fig. 6) has the effect of short-circuiting the current originating from the surface, making the thickness of the layer impossible to ascertain. From Fig. 6 we can only conclude that the layer is either continuous (ERT4) or discontinuous (ERT1).

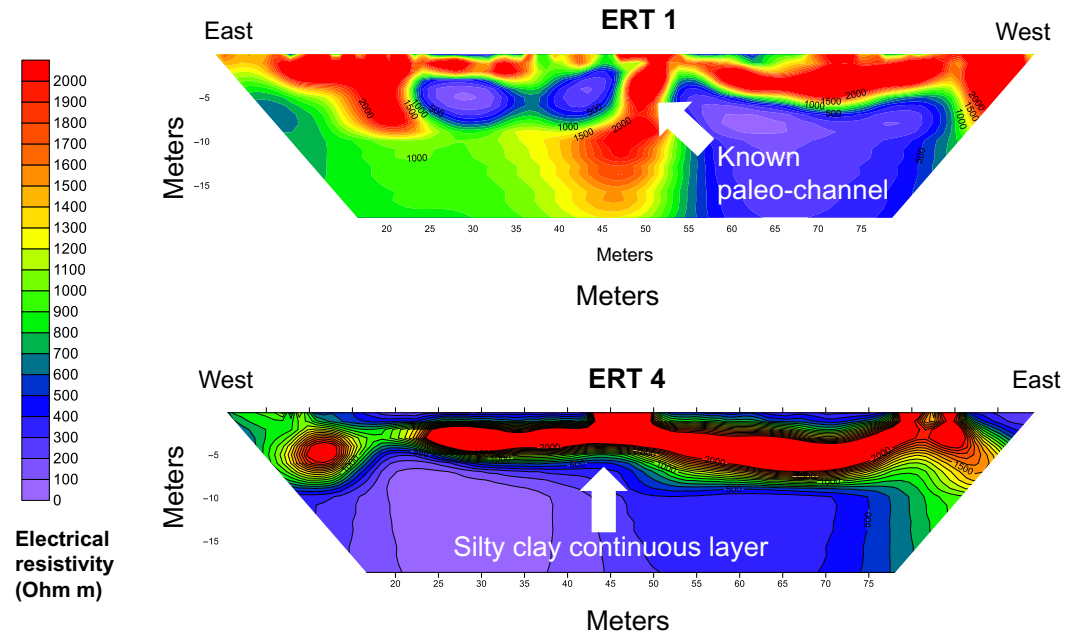

FIG. 6 Aviano site: two ERT lines showing, respectively, one or more discontinuities in the clay layer (ERT1 above) and its continuity (ERT4). See discussion in the text.

Fig. 7 shows the result of a cross-hole ERT survey conducted between two purposely installed boreholes roughly mid-way along line ERT4: on the left the stratigraphic log shows that the clay layer is here only about 0.5 m thick. The cross-hole ERT uses 48 electrodes, 24 in each hole at the side of the section. The electrodes are spaced at 0.8 m along each borehole. The acquisition scheme is a dipole–dipole skip 4 configuration (i.e., the current and potential dipoles are $6 \times 0.8 = 4.8$ m long) and a full reciprocal acquisition. The inversion is again performed using the Occam's inversion R2t freeware by A. Binley. Note how the electrically conductive layer is well marked, and the resistive gravels below are well visible, unlike in Fig. 6. The conductive anomaly, however, is thicker than the clay layer per se, as it incorporates also the perched aquifer above the clay layer.

3.1.4 *The Fondo Paviani site*

The Fondo Paviani site, located near Legnago, Verona, Italy, is an embanked settlement extending over several hectares, dating back to the Late Bronze Age (Cupitò et al., 2015). The site is now largely covered by crops, and the investigation of its structure thus requires extensive nondestructive investigations. Fig. 8 shows the results of preliminary investigations at the site performed using a combination of EMI mapping and ERT lines. In particular, at this site we successfully tested the EMI inversion procedure described by Deidda et al. (2014, 2017). Data were acquired using a multifrequency conductivity meter GEM-2 by Geophex, with a total seven frequencies in the frequency range from 775 Hz and 47 kHz. The instrument

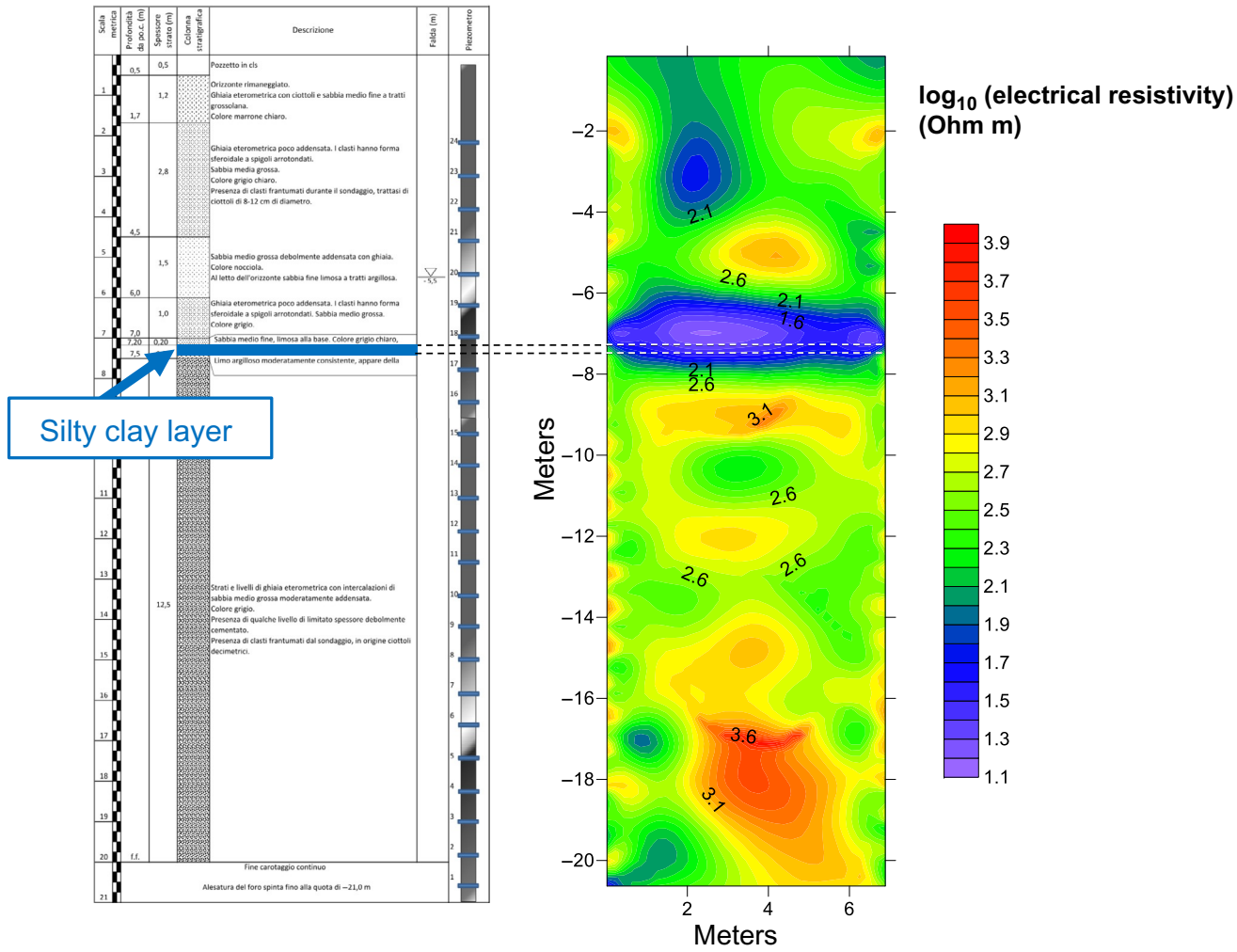

FIG. 7 Aviano site: cross-hole ERT imaging. See text for a discussion.

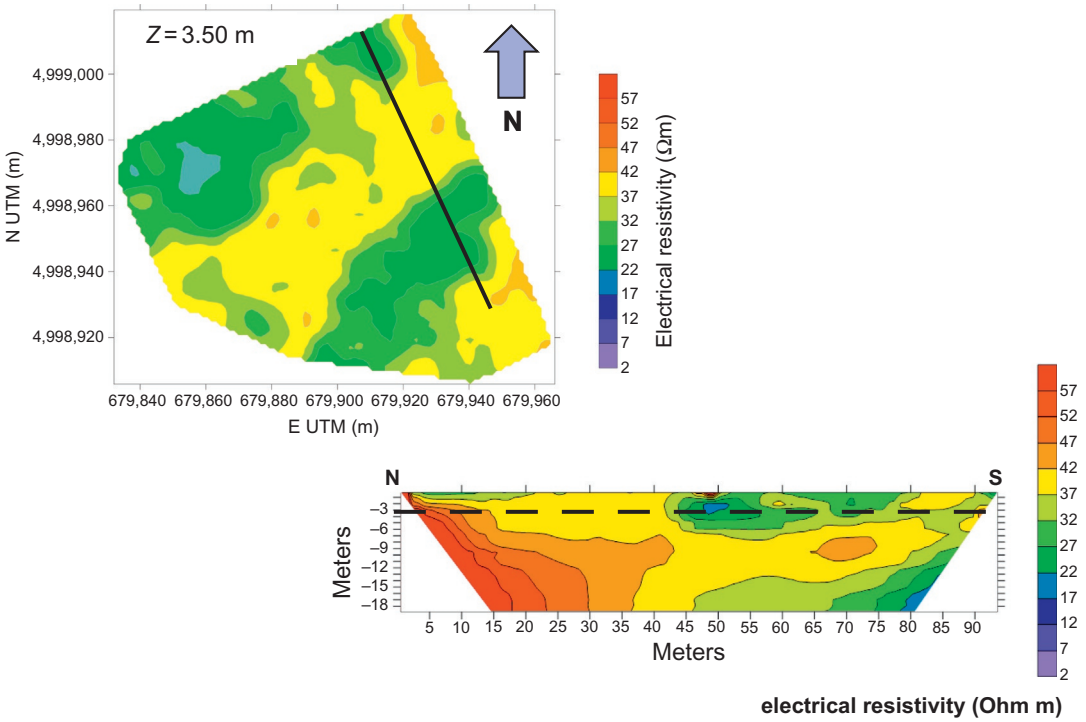

FIG. 8 Fondo Paviani site: comparison between EMI inverted results at 3.5 m depth and the corresponding ERT line. See text for details and discussion.

is equipped with a differential GPS for automatic positioning, so that a 3D volume of electrical conductivity can be obtained from the 1D vertical inverted profiles. We also acquired several ERT profiles in the same area using an Iris Instrument Syscal Pro with a dipole–dipole skip 4 configuration and a full reciprocal acquisition. ERT inversion was performed using the freeware ProfileR by A. Binley (see above).

The comparison shown in Fig. 8 shows how the EMI inverted data are totally comparable with the ERT results, and are extremely advantageous in terms of speed of acquisition, and consequently the spatial coverage can be much larger. Similar successful results are also described, e.g., in Boaga et al. (2018).

3.1.5 *The Turriaco site*

The Turriaco site is located in the Friuli region (NE Italy) on the hydrographic left side of the Isonzo River. The study was designed to explore the characteristics of the Isonzo riparian zone. Here we present some results in terms of seismic characterization—note that other data, including ERT, were collected at the site. For a thorough description see Vignoli et al. (2016).

From a lithological point of view, the site is a heterogeneous sequence of quaternary sediments mainly consisting of gravel with different contents of sand and silt originated

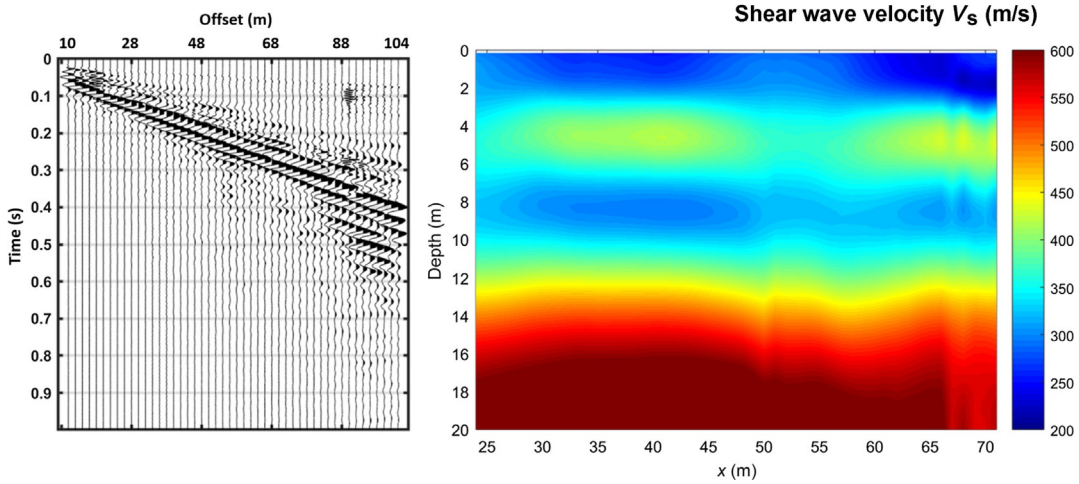

FIG. 9 Turriaco site: results of the sMOPA inversion of Rayleigh waves (*right*) starting from a suite of shots along the line (an example on the *left*). See text for details.

by Alpine erosion. The braided nature of the Isonzo River partly accounts for the heterogeneous nature of the sediments. The subsoil is an alternate sequence of facies with high (gravel and sand) and low hydraulic conductivity (clay and silt). Here we discuss some unpublished results concerning seismic acquisition and surface wave inversion. The seismic signals were generated by a sledgehammer and recorded by means of a Geode seismograph (Geometrics Inc.) using arrays of 48 4.5-Hz geophones spaced 2 m. Multiple shots were acquired along each line and processed as described in Vignoli et al. (2011). Results of the sMOPA inversion for one of the lines are shown in Fig. 9 together with a sample shot. The procedure is capable of producing a 2D profile of shear wave velocity with no need for lateral a priori constraints, which are frequently unjustified.

3.2 Fluid dynamics monitoring

3.2.1 The Decimomannu site

The Decimomannu military air base is located in Southern Sardinia, Italy, a few km north of Cagliari. Some instances of soil contamination have been observed recently as a consequence of three known spills of jet fuel (JP8) from supply pipelines. Several containment and remediation activities have been in place for some years. Now, novel in situ remediation actions are being planned. Here we present the preliminary results of noninvasive monitoring of feasibility injection tests. Two different solutions were injected in sequence over a few hours. We used a fixed ERT line composed of 48 electrodes spaced at 1 m. The scheme was a dipole–dipole skip zero (i.e., with dipoles having the minimal size of 1 m) with full reciprocal acquisition. Inversion is based on the ratio inversion approach (see, e.g., Cassiani et al., 2006) using the profileR freeware by A. Binley.

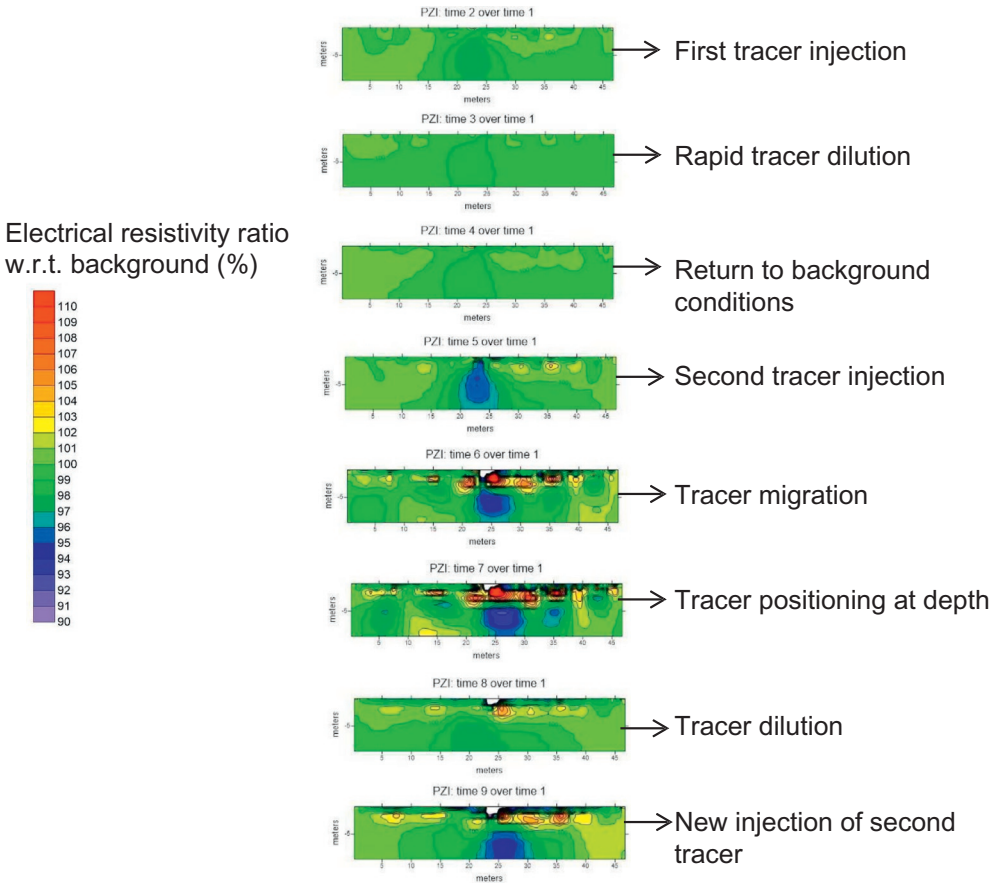

FIG. 10 Decimomannu site: time-lapse surface ERT measurements show the extent and migration of fluids injected for contaminant remediation. See text for details.

Fig. 10 shows the time-lapse results of the monitoring: the injection borehole is located at the center of the monitoring line. The entire sequence lasts for only a few hours. The results are presented as resistivity ratio with respect to background conditions, reported as a percentage. It is apparent that both injected solutions are visible in terms of electrical resistivity reduction, even though the first solution is clearly less conductive than the second. It is crucial to know where the injected solution moves in terms of invasion of the contaminated zone if an effective remediation strategy is to be implemented.

3.2.2 *The Trento Nord site*

The site is located in the city of Trento, Trentino Province (NE Italy). Since the early 1900s the area housed important chemical industries that left a legacy of heavy contamination, particularly in terms of organic compounds. Among others techniques, in situ ozonation was

selected as the most efficient method to remediate soil and groundwater pollution, due to the high capability of ozone to oxidize organic contaminants to safe levels. In a very permeable matrix, in situ ozone hydrocarbon oxidation is very successful; in the presence of relatively low permeability soils, as is the case of the considered site, the treatment may instead be long and costly. For this reason, hydraulic fracturing by means of pressurized water has been tested in conjunction with ozonation. A preliminary phase of hydraulic fracturing testing was performed to assess the best water injection rate and pressure values. The fluid used for hydraulic fracturing was a nearly saturated NaCl brine, the arrival of which in nearby boreholes is traditionally monitored via downhole electrical conductivity meters. Cross-borehole ERT was proposed and implemented as an additional imaging technique to assess the effectiveness of brine migration following fracturing. This monitoring was proposed because ERT is known to be very sensitive to conductivity contrasts at depth. The measurement scheme was composed of a dipole–dipole skip 1 (AB-MN) and a cross-hole bipole (AM-BN) configurations, using a total of only 259 electrodes combinations. Note that while each cable had 24 electrodes, only 30 of the 48 electrodes were actually utilized, as the water level was at about 3.6 m below ground.

Hereafter we present the results of the time-lapse ERT imaging during the preliminary fracturing tests (Fig. 11). Note that the injection chamber was placed in the injection hole (borehole 0 in Fig. 11)—approximately between 7.5 and 8 m, i.e., in the sand-with-gravel formation. The high injection pressure, however, clearly moved the brine upward, fracturing the silt (a desired result). This is confirmed by the time-lapse ERT data. Note that the ERT results are heavily affected in this case by the so-called *borehole effect*: the brine invasion of the boreholes where the electrodes are placed produces artifacts. Higher resistivity than background appears in the regions near the boreholes—a consequence of the short-circuiting within the brine-invaded boreholes themselves. Nevertheless, the results are very informative in practical terms.

3.2.3 The Grugliasco site

The Grugliasco site is in the campus of the Agricultural Faculty of the University of Turin, Italy. The soil in this area is largely made of aeolian sands. The unsaturated zone has a porosity ranging between 0.35 and 0.4, high vertical permeability, and low organic content; therefore, the area represents an ideal test site for percolation studies. The water table is at about 20-m depth. A full description of the site can be found elsewhere (Cassiani, et al., 2009c; Manoli et al., 2015; Rossi et al., 2015; Raffelli et al., 2017). An irrigation experiment was performed at the site on September 28, 2004 by means of a line of sprayers, placed in the middle of the experimental area, in order to wet an area of about 3 m by 20 m completely. The soil was initially extremely dry as a consequence of an exceptionally dry summer period.

We performed time-lapse surface-to-surface GPR monitoring during the experiment using a PulseEkko 100 radar system with 200 MHz antennas in wide-angle reflection and refraction (WARR) configuration, i.e., keeping the transmitter fixed and moving the receiver with offset increments equal to 10 cm over a 14-m line. A GPR WARR survey was acquired before the start of irrigation, and then roughly every 2 h over the 6-h irrigation period. Fig. 12 shows the corresponding four WARR GPR images. Here we present a simple interpretation based on classical critical refraction theory, albeit other more sophisticated approaches are possible

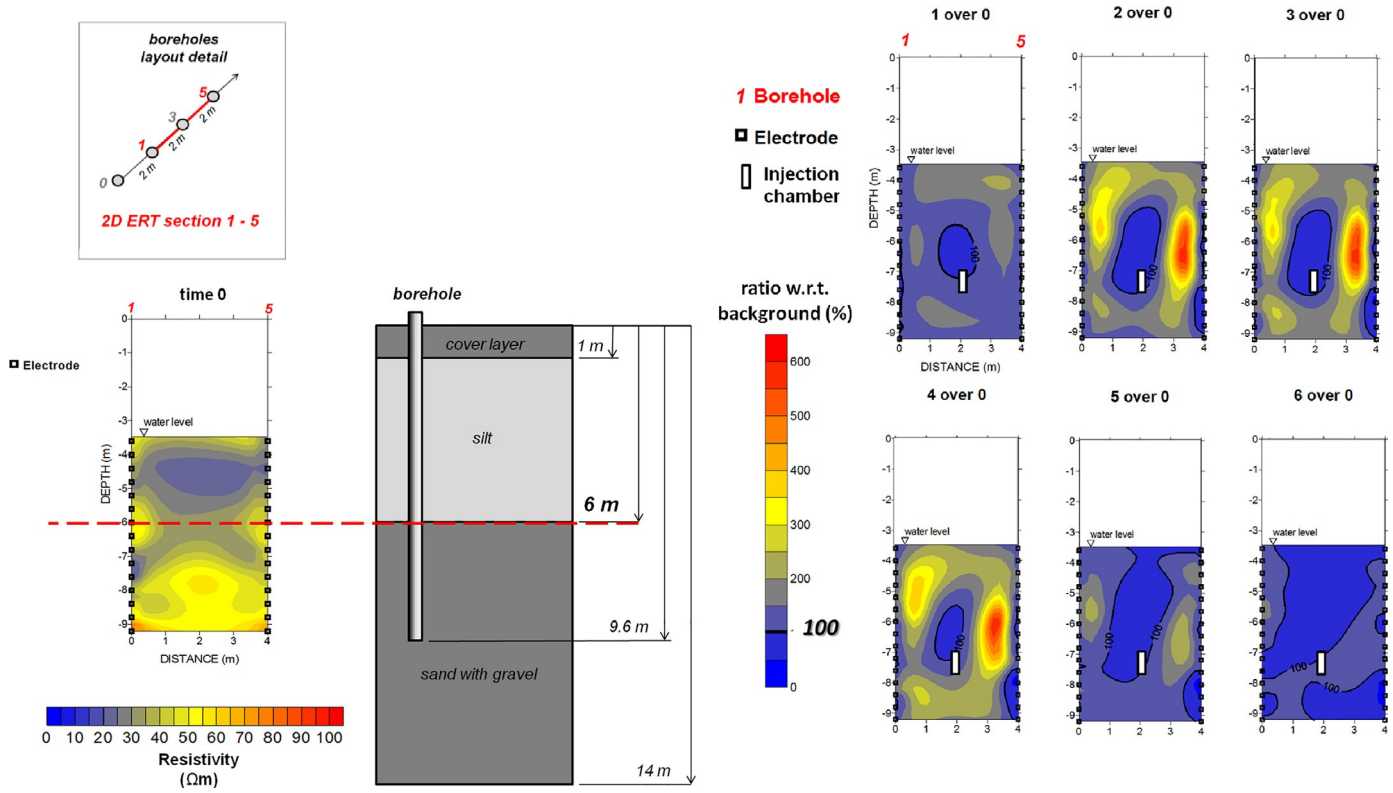

FIG. 11 Trento Nord site. Left: background cross-hole ERT image compared against the local lithological profile (from drilling). Right: time-lapse images of resistivity changes as % ratios with respect to background conditions. See text for details and discussion.

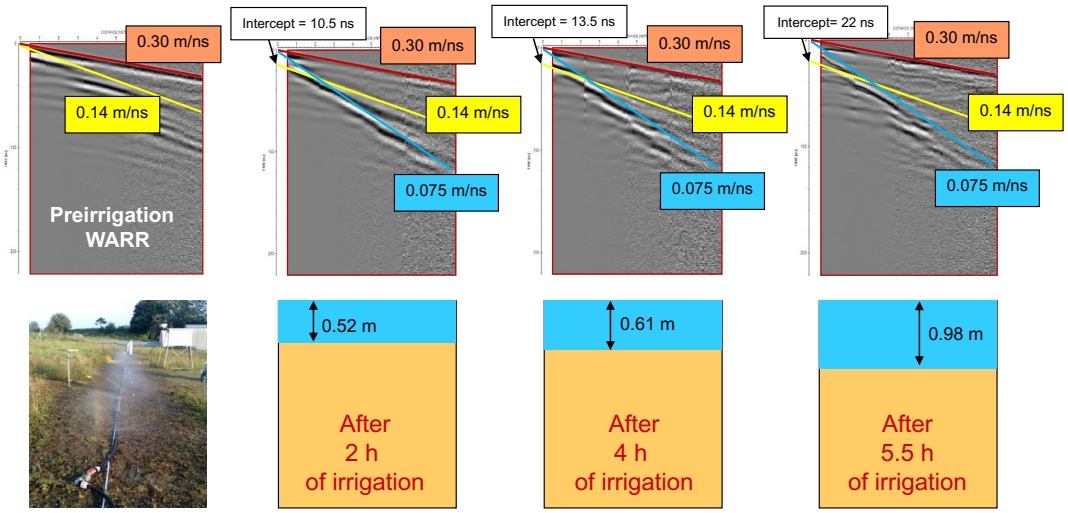

FIG. 12 Grugliasco site: time-lapse GPR WARR data during an infiltration experiment (*above*) and corresponding interpretation in terms of refraction analysis (*below*). See text for details and discussion.

based on guided wave analysis (Strobbia and Cassiani, 2007; Rossi et al., 2015). As a result, the infiltration speed is estimated directly from the GPR WARR data—a procedure described by van Overmeeren et al. (1997).

3.2.4 The Bregonze site

The Bregonze experimental site is located in a pre-Alpine area, north of Vicenza (North-Eastern Italy)—for a full description see Vignoli et al. (2012). The area of interest is the headwater catchment drained by an ephemeral stream, characterized by roughly 1.5 ha (about 200 m long and 100 m wide, altitude from 375 to 395 a.m.s.l.) and very mild slopes (~7.5%). From a geological point of view, the site is composed of Upper Paleocene-Holocene altered volcanic deposits, with a strong clayey component. The soil, down to about 1–1.5 m, is of a silty-clay nature with average weight fractions equal to 21% sand and 79% silt+clay, and an organic matter content around 13%. Given the very low hydraulic conductivity of the deeper subsoil, this upper soil layer controls the site's hydrology. Therefore, monitoring of the volumetric soil moisture content is particularly important at this site in order to help calibrate full scale hydrological models (e.g., Weill et al., 2013). We used a GF Instruments CMD electro-magnetometer with different configurations. Fig. 13 shows the maps obtained using the CMD1 configuration with vertical loops, with a depth of investigation around 1.5 m. Note that the mapped quantity is the apparent electrical resistivity within this 1.5 m thickness, which we calculate using an average value. Measureable changes are apparent in less than 2 months. Similar results have been observed by a number of authors (e.g., Robinson et al., 2007).

3.2.5 The Bari IRSA-CNR site

This is an experimental site located in the IRSA-CNR headquarters in Bari, Apulia (Southern Italy). The site geology is characterized, from top to bottom, by a relatively thin soil layer (1.5 m) followed by a 5-m thick layer of calcarenite, a sedimentary carbonatic rock

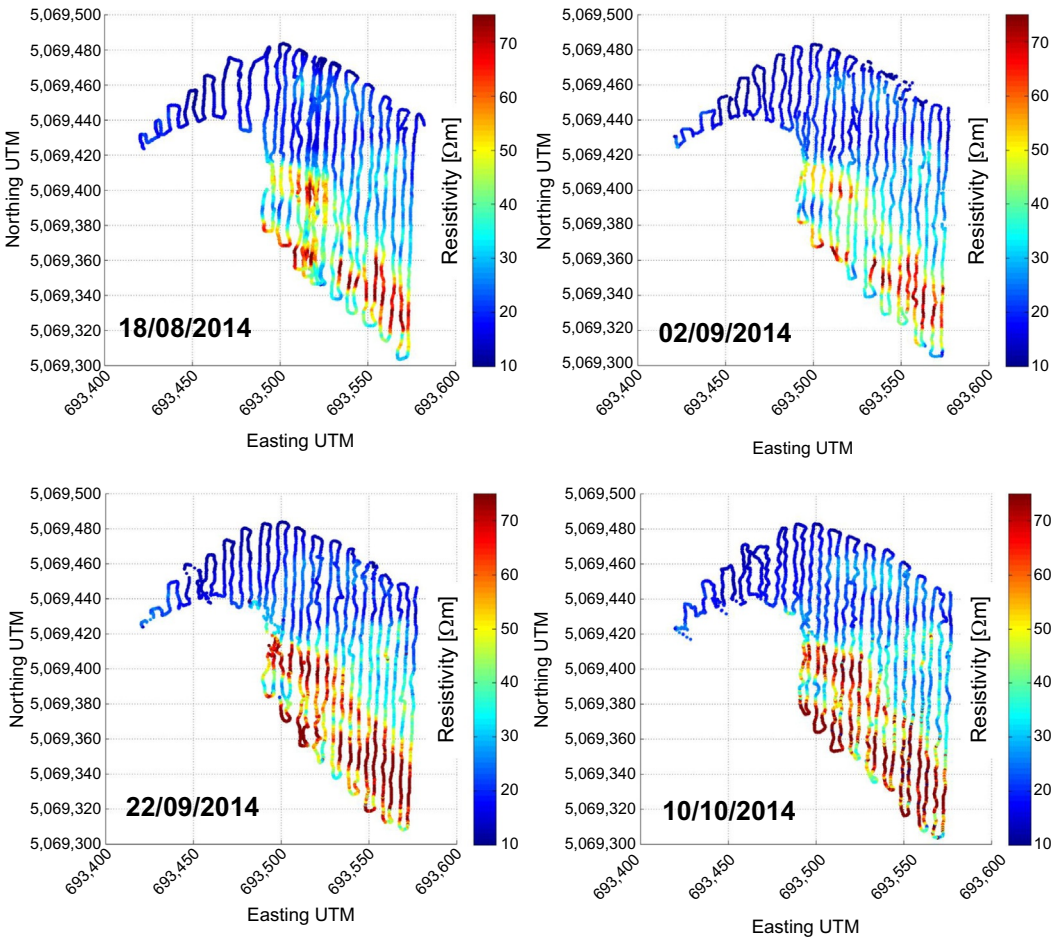

FIG. 13 Bregonze site: time-lapse maps of apparent electrical resistivity as obtained from EMI measurements—note the changes over time. See text for a discussion.

of marine origin of Plio-Pleistocene age. Calcarenite is a porous rock, slightly cemented, made of a granular skeleton and carbonatic cement. The calcarenite formation lies on top of a karstic fractured limestone, about 25 m thick, that constitutes the aquifer. The water table is located in this formation. At greater depths, the wells encounter a dolomitic limestone about 20 m thick.

We conducted an infiltration experiment, conceptually similar to the ones described by Deiana et al. (2007, 2008). A 1.5-m deep trench was dug to allow water infiltration into the underlying calcarenite between the existing boreholes C and E, and a mildly saline aqueous solution was used as a tracer in order to be potentially visible both above and below the water table. About 20 m^3 of water were injected in 4 h, from 14:30 to 18:30 on March 17, 2010. A combination of cross-hole multiple offset gather GPR, vertical radar profiles, and surface electrical resistivity tomography (ERT) was used to monitor in time-lapse mode the dynamics of the vadose zone, while the deeper part of the profile was imaged

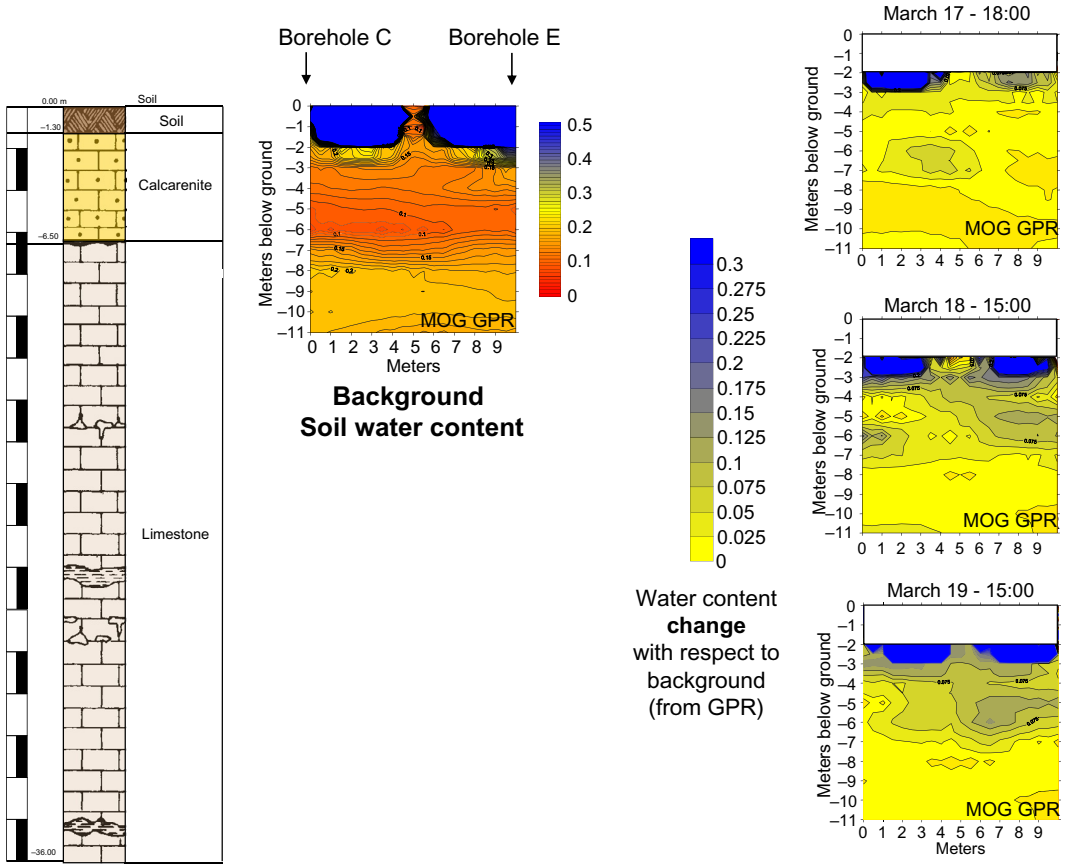

FIG. 14 Bari IRSA-CNR site. *Left*: background conditions as imaged using multiple offset gather (MOG) GPR tomography (converted to moisture content using Topp et al., 1980), compared against borehole stratigraphy. *Right*: time lapse changes following the trench infiltration experiment.

using cross-hole time-lapse ERT. The monitoring results are potentially useful as calibration data for a variably saturated flow and transport model.

Here we focus on the MOG GPR data (Fig. 14). A substantial delay is observed in the vertical migration of water, probably due to fast initial lateral spreading.

4 Future challenges and conclusions

The use of noninvasive techniques for subsoil characterization is now well established across many application areas. Despite this, the increasing use of such techniques for shallow applications, of direct environmental interest, has posed formidable challenges over the past three decades. Many such challenges have been overcome, as shown earlier. Yet the main issue that remains is to disseminate these techniques to a wider audience that is still reluctant to apply the latest techniques. There are luckily many exceptions. For instance, the hydrological community has been an eager adopter of shallow imaging: it is very common to see papers and presentations where standard hydrologists use and comment geophysical results

(hydro-geophysical in that case) as part of their own toolbox. This an extraordinary success. Other communities are more difficult to penetrate. But it is only a matter of time and commitment: geophysicists must learn to sell their results in a manner that is easy to digest for end users, and must learn from end users what their actual needs are (see Fig. 2) in order to devise the best approaches to answer their practical questions. As geophysics, and near-surface geophysics in particular, is a frontier discipline, we (geophysicists) must learn to communicate more and better knowing that the value of the information we can provide is much higher than currently felt outside of our field.

Of course, a number of advances can and should also be made. We envision quite a few areas of promising progress, in no particular order, mixing techniques and applications:

- EMI inversion: the availability of EMI instruments that can collect multifrequency or multi-coil data opens a wide range of possibilities in terms of inverting (at least in vertical 1D) the EMI data and ultimately obtaining 3D volumes of electrical conductivity. Such techniques can also be used in time series. The advantage of this method is that the measured quantity is the same as that measured by ERT but it can be used as a finer resolution/detailed investigation, and can be used to complement traditional ERT data collection. See, among others, the recent application by Boaga et al. (2018) and von Hebel et al. (2018).
- Advanced analysis of seismic surface waves: even though the physics have been well understood for many years, there remains much work to be done to bring surface wave (SW) investigations to a mature stage. In particular, the analysis of phase dependence versus offset, also taking into account the multimodal propagation of SWs, is the path forward to devise 2D and 3D tomographic techniques. The future of SW is brilliant, and will complement all other near-surface techniques, where classical reflection and refraction seismics still play too minor a role. The reader can follow developments along this line the pioneering work of Strobbia and Foti (2006), Vignoli and Cassiani (2010), Vignoli et al. (2011, 2012, 2016) and others to come.
- Airborne EMI and TDEM in particular: the noncontact characteristics of EMI measurements paves the way to a number of exciting developments, especially when coupled with EMI inversion techniques (see above). Helicopter-based TDEM investigations are now state-of-the-art (e.g., Viezzoli et al., 2008); smaller scale applications are conceivable (e.g., using drones).
- IP/SIP quantitative interpretation: while IP has been around for many years, and substantial effort has been expended to attach a physical explanation to its response, in a wide range of applications (consider, e.g., Kemna et al., 2004; Lesmes and Friedman, 2005; Binley et al., 2005; Ntarlagiannis et al., 2006; Cassiani et al., 2009a, 2009b; Kemna et al., 2012), there is still quite some way to go before one can safely interpret IP data in more than a pure "imaging" sense. Yet, IP and SIP in particular contain information that comes from aspects of the subsurface that are otherwise impossible to explore, with special reference to the properties of porous media inner interfaces, and the relevant links to permeability, grain size distribution, contamination, and other properties. Thus, we expect IP/SIP to be the object of long-term exciting research.
- SP (spontaneous potential): somehow, SP has suffered the same ups and downs as IP/SIP: like IP/SIP, a true and honest quantitative interpretation of the SP technique is still difficult, despite loud claims of success in the past. Nevertheless, SP clearly carries information, and shall be further exploited (see, e.g., Naudet et al., 2003).

- Surface nuclear magnetic resonance (SNMR): while NMR is state of the art in medical imaging (as much as X-ray, CT), its use in subsurface investigations is still lagging behind, in spite of promising results (e.g., Braun et al., 2009). This is not so much due to theoretical issues, but instead because the measurable signal is very small under field conditions, so as to be overwhelmed, e.g., in urban areas. Yet, SNMR measures properties that cannot be measured otherwise, with particular emphasis on "free water," and thus permeability. Potentially there are big advances to make, yet if the ultimate limitations will be proven to be in the physics, this might be a dead end.
- Gravimetry: this is a very old technique, and often used for large-scale characterization. However, the precision of modern instruments easily extend into the microGal range. In addition, time-lapse measurements have been proven to detect changes in mass associated with water storage at a variety of scales, from the local to the regional scale (e.g., Biegert et al., 2008). Coupling with hydrological modeling is straightforward, and may open unexpected opportunities (e.g., Piccolroaz et al., 2015).
- Very small scale applications, e.g., agricultural applications (plant roots): the scale of investigation of some techniques (particularly EMI and ERT) can be made small enough to investigate the subsurface in the region of practical and scientific interest for the biosphere. The concepts of the Earth's critical zone and that of the soil–plant-atmosphere continuum have long been introduced in order to define areas of extremely high importance in a variety of natural sciences: the interface between the solid planet and its atmosphere is key to a number of vital processes, and all involve mass and energy transfer. At this scale, noninvasive techniques may prove invaluable, and major progresses are being made (e.g., Allred et al., 2008; Petersen and Al Hagrey, 2009; Cassiani et al., 2012, 2015, 2016; Consoli et al., 2017; Vanella et al., 2018; Mary et al., 2018, to mention a few).
- The link to contamination: it should always be remembered that contamination can be dangerous, or even deadly, at concentrations that are so small as not to produce any physical signal (and indeed, concentrations are measured by chemical methods). Thus, it may sound overambitious to expect geophysical methods to be able to detect contamination. Yet, geophysics may identify side effects. If these effects can be disentangled from other signal sources (typically, structure and dynamics) then it is possible to relate noninvasive measurements to contaminant distributions (e.g., Kästner et al., 2012; Cassiani et al., 2014).
- Data assimilation into models: modeling of processes means understanding processes. Ultimately, this is the final goal of any scientific process, including subsoil investigations. Thus major efforts shall be expended to try and blend data, and noninvasive data, with models. This can be done by ad hoc analyses (e.g., Preti et al., 2018; Robinson et al., 2007) or in a strict sense (e.g., Manoli et al., 2015; Camporese et al., 2011, 2015). Either way, this is at the heart of the scientific method, so any progress in this direction is welcome.
- Last but not least, technological progresses: for instance, optical fiber measurements of seismic waves. Another possibility is directional drilling to place electrodes or optical fibers in the subsoil (Fig. 15, Busato et al., 2018). Distributed sensors (temperature, vibrations, etc.) in integrated circuits (e.g., MEMS) are also promising. The range of possibilities is immense.

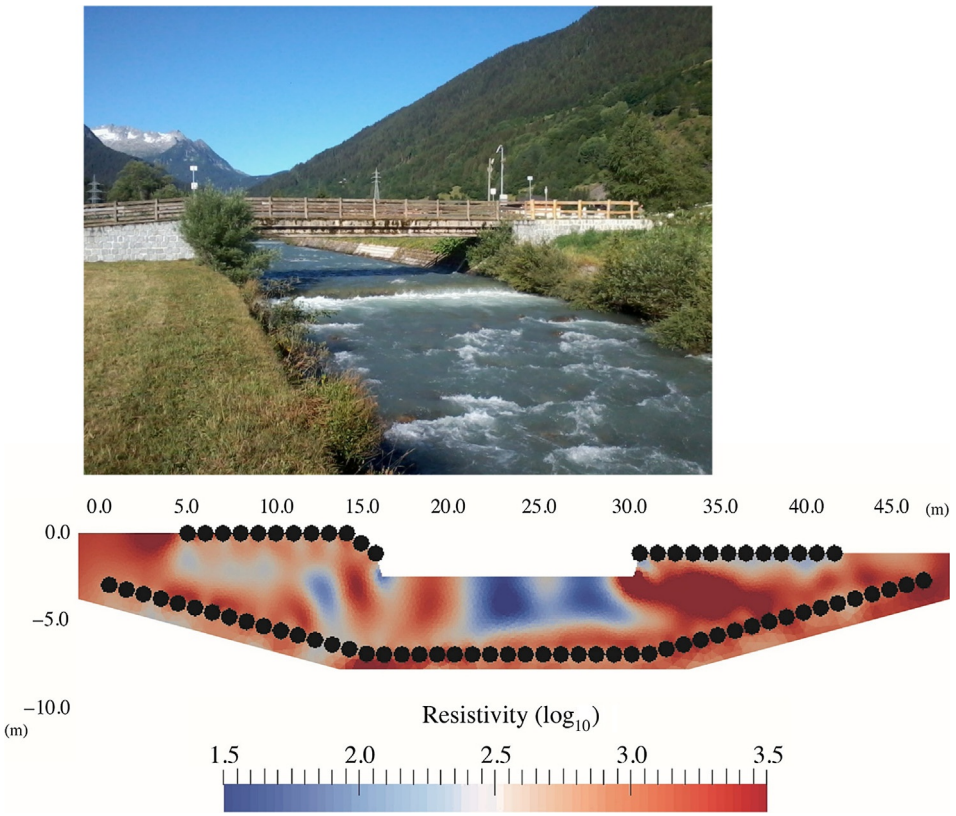

FIG. 15 Vermigliana site: ERT imaging of the hyporheic zone made possible by directional drilling electrode placement below the river bed (Busato et al., 2018).

Acknowledgments

We are in debt with countless people, who helped develop both the general view presented in this chapter, and the specific results we described in the case studies. As we cannot acknowledge all, admitting the risk of forgetting some, we play it safe and thank Professor Andrew M. Binley, whose example has been a reference for all of us, and whose continuous and dedicated efforts have made the discipline progress beyond expectations. He is a sincere friend for many of us.

References

Aki, K., Richards, P.G., 2002. Quantitative Seismology, second ed. University Science.

Allred, B.J., Daniels, J.J., Ehsani, M.R., 2008. Handbook of agricultural geophysics. CRC Press, Taylor and Francis Group, New York.

Alumbaugh, D., Chang, P.Y., Paprock, L.I., Brainard, I.R., Glass, R.J., Rautman, C.A., 2002. Estimating moisture contents in the vadose zone using cross-borehole ground penetrating radar: a study of accuracy and repeatability. Water Resour. Res. 38, 1309. https://doi.org/10.1029/2001WR000754.

Annan, A.P., 2005. GPR methods for hydrogeological studies. In: Rubin, Y., Hubbard, S.S. (Eds.), Hydrogeophysics, Ser. In: vol. 50. Springer, Dordrecht, pp. 185–214.

Archie, G.E., 1942. The electrical resistivity log as an aid in determining some reservoir characteristics. Trans. AIME 146, 54–62.

Arcone, S.A., 1984. Field observations of electromagnetic pulse propagation in dielectric slabs. Geophysics 49, 1763–1773.

Arcone, S.A., Peapples, P.R., Liu, L., 2003. Propagation of a ground-penetrating radar (GPR) pulse in a thin surface waveguide. Geophysics 68, 1922–1933.

Auken, E., Christiansen, A.V., Kirkegaard, C., Fiandaca, G., Schamper, C., Behroozmand, A., Binley, A., Nielsen, E., Effersø, F., Christensen, N., Sørensen, K., Foged, N., Vignoli, G., 2015. An overview of a highly versatile forward and stable inverse algorithm for airborne, ground-based and borehole electromagnetic and electric data. Explor. Geophys. 46 (3), 223–235. https://doi.org/10.1071/EG13097.

Bevc, D., Morrison, H.F., 1991. Borehole-to-surface electrical resistivity monitoring of a salt water injection experiment. Geophysics 56, 769–777.

Biegert, E., Ferguson, J., Li, X., 2008. 4D gravity monitoring—Introduction. Geophysics 73. https://doi.org/10.1190/1.3010377. Special Section—4D gravity monitoring, WA1 (2008).

Binley, A., Beven, K., 2003. Vadose zone flow model uncertainty as conditioned on geophysical data. Ground Water 41, 119–127.

Binley, A.M., Cassiani, G., Middleton, R., Winship, P., 2002a. Vadose zone flow model parameterisation using cross-borehole radar and resistivity imaging. J. Hydrol. 267, 147–159.

Binley, A., Henry-Poulter, S., Shaw, B., 1996. Examination of solute transport in an undisturbed soil column using electrical resistance tomography. Water Resour. Res. 32, 763–769.

Binley, A.M., Kemna, A., 2005. DC resistivity and induced polarization methods. In: Rubin, Y., Hubbard, S.S. (Eds.), Hydrogeophysics. Water Sci. Technol. Library, Ser. In: vol. 50. Springer, New York, pp. 129–156.

Binley, A., Ramirez, A., Daily, W., 1995. Regularised image reconstruction of noisy electrical resistance tomography data. In: Beck, M.S., Hoyle, B.S., Morris, M.A., Waterfall, R.C., Williams, R.A. (Eds.), Process Tomography—1995, Proceedings of the fourth Workshop of the European Concerted Action on Process Tomography, Bergen, 6–8 April 1995, pp. 401–410.

Binley, A.M., Slater, L.D., Fukes, M., Cassiani, G., 2005. The relationship between frequency dependent electrical resistivity and hydraulic properties of saturated and unsaturated sandstone. Water Resour. Res. 41. https://doi.org/10.1029/2005WR004202.

Binley, A., Winship, P., West, L.J., Pokar, M., Middleton, R., 2002b. Seasonal variation of moisture content in unsaturated sandstone inferred from borehole radar and resistivity profiles. J. Hydrol. 267, 160–172.

Boaga, J., Ghinassi, M., D'Alpaos, A., Deidda, G.P., Rodriguez, G., Cassiani, G., 2018. Geophysical investigations unravel the vestiges of ancient meandering channels and their dynamics in tidal landscapes. Sci. Rep. 8, 1–8. ISSN: 2045–2322. https://doi.org/10.1038/s41598-018-20061-5.

Braun, M., Kamm, J., Yaramanci, U., 2009. Simultaneous inversion of magnetic resonance sounding in terms of water content, resistivity and decay times. Near Surf. Geophys. 7, 589–598.

Brovelli, A., Cassiani, G., 2010. A combination of the Hashin-Shtrikman bounds aimed at modelling electrical conductivity and permittivity of variably saturated porous media. Geophys. J. Int. 180, 225–237. https://doi.org/10.1111/j.1365-246X.2009.04415.x.

Brovelli, A., Cassiani, G., Dalla, E., Bergamini, F., Pitea, D., Binley, A.M., 2005. Electrical properties of partially saturated sandstones: a novel computational approach with hydro-geophysical applications. Water Resour. Res.. 41. https://doi.org/10.1029/2004WR003628.

Burbery, L., Cassiani, G., Andreotti, G., Ricchiuto, T., Semple, K.T., 2004. Well test and stable isotope analysis for the determination of sulphate-reducing activity in a fast aquifer contaminated by hydrocarbons. Environ. Pollut. 129 (2), 321–330.

Busato, L., Boaga, J., Perri, M.T., Majone, B., Bellin, A., Cassiani, G., 2018. Hydrogeophysical characterization and monitoring of the hyporheic and riparian zones: the Vermigliana Creek case study. Sci. Total Environ. 648, 1105–1120. https://doi.org/10.1016/j.scitotenv.2018.08.179.

Camporese, M., Cassiani, G., Deiana, R., Salandin, P., Binley, A., 2015. Coupled and uncoupled hydrogeophysical inversions using ensemble Kalman filter assimilation of ERT-monitored tracer test data. Water Resour. Res. 51 (5), 3277–3291. https://doi.org/10.1002/2014WR016017.

Camporese, M., Salandin, P., Cassiani, G., Deiana, R., 2011. Assessment of local hydraulic properties from electrical resistivity tomography monitoring of a three-dimensional synthetic tracer test experiment. Water Resour. Res. 47. https://doi.org/10.1029/2011WR010528.

Cassiani, G., Binley, A.M., 2005. Modeling unsaturated flow in a layered formation under quasi-steady state conditions using geophysical data constraints. Adv. Water Resour. 28, 467–477.

Cassiani, G., Binley, A., Kemna, A., Wehrer, M., Flores Orozco, A., Deiana, R., Boaga, J., Rossi, M., Dietrich, P., Werban, U., Zschornack, L., Godio, A., JafarGamdomi, A., Deidda, G.P., 2014. Non-invasive characterization of the Trecate (Italy) crude-oil contaminated site: links between contamination and geophysical signals. Environ. Sci. Pollut. Res. 21 (15), 8914–8931. https://doi.org/10.1007/s11356-014-2494-7. Special Issue on "New approaches for low-invasive contaminated site characterization, monitoring and modelling".

Cassiani, G., Boaga, J., Rossi, M., Fadda, G., Putti, M., Majone, B., Bellin, A., 2016. Soil-plant interaction monitoring: small scale example of an apple orchard in Trentino, North-Eastern Italy. Sci. Total Environ. 543 (Pt B), 851–861. https://doi.org/10.1016/j.scitotenv.2015.03.113.

Cassiani, G., Boaga, J., Vanella, D., Perri, M.T., Consoli, S., 2015. Monitoring and modelling of soil-plant interactions: the joint use of ERT, sap flow and Eddy Covariance data to characterize the volume of an orange tree root zone. Hydrol. Earth Syst. Sci. 19, 2213–2225. https://doi.org/10.5194/hess-19-2213-2015.

Cassiani, G., Bruno, V., Villa, A., Fusi, N., Binley, A.M., 2006. A saline tracer test monitored via time-lapse surface electrical resistivity tomography. J. Appl. Geophys. 59, 244–259.

Cassiani, G., Godio, A., Stocco, S., Villa, A., Deiana, R., Frattini, P., Rossi, M., 2009a. Monitoring the hydrologic behaviour of steep slopes via time-lapse electrical resistivity tomography. Near Surf. Geophys. 475–486. special issue on Hydrogeophysics.

Cassiani, G., Kemna, A., Villa, A., Zimmermann, E., 2009b. Spectral induced polarization for the characterization of free-phase hydrocarbon contamination in sediments with low clay content. Near Surf. Geophys. 547–562. https://doi.org/10.3997/1873-0604.2009028. special issue on Hydrogeophysics—Methods and Processes.

Cassiani, G., Ferraris, S., Giustiniani, M., Deiana, R., Strobbia, C., 2009c. Time-lapse surface-to-surface GPR measurements to monitor a controlled infiltration experiment. Boll. Geofis. Teor. Appl. 50 (2), 209–226.

Cassiani, G., Fusi, N., Susanni, D., Deiana, R., 2008. Vertical radar profiles for the assessment of landfill capping effectiveness. Near Surf. Geophys. 6, 133–142.

Cassiani, G., Strobbia, C., Gallotti, L., 2004. Vertical radar profiles for the characterization of the deep vadose zone. Vadose Zone J. 3, 1093–1115.

Cassiani, G., Ursino, N., Deiana, R., Vignoli, G., Boaga, J., Rossi, M., Perri, M.T., Blaschek, M., Duttmann, R., Meyer, S., Ludwig, R., Soddu, A., Dietrich, P., Werban, U., 2012. Non-invasive monitoring of soil static characteristics and dynamic states: a case study highlighting vegetation effects. Vadose Zone J. 11, https://doi.org/10.2136/2011.0195. Special Issue on SPAC—Soil-plant interactions from local to landscape scale. vzj2011.0195.

Christiansen, A.V., Auken, E., Sørensen, K., 2006. The transient electromagnetic method. In: Kirsch, R. (Ed.), Groundwater Geophysics: A Tool for Hydrogeology. Springer-Verlag, Berlin, pp. 179–224.

Consoli, S., Stagno, F., Vanella, D., Boaga, J., Cassiani, G., Roccuzzo, G., 2017. Partial root-drying irrigation in orange orchards: effects on water use and crop production characteristics. Eur. J. Agron. 82, 190–202. https://doi.org/10.1016/j.eja.2016.11.001.

Crook, N., Binley, A., Knight, R., Robinson, D.A., Zarnetske, J., Haggerty, R., 2008. Electrical resistivity imaging of the architecture of sub-stream sediments. Water Resour. Res. 44. https://doi.org/10.1029/2008WR006968.

Cupitò, M., Leonardi, G., Dalla Longa, E., Nicosia, C., Balista, C., Dal Corso, M., Kirleis, W., 2015. Fondo Paviani (Legnago, Verona): il central place della polity delle Valli Grandi Veronesi nella tarda Età del bronzo. Cronologia, aspetti culturali, evoluzione delle strutture e trasformazioni paleoambientali. In: del Veneto, P.e.P., Leonardi, G., Tiné, V. (Eds.), Studi di preistoria e protostoria -2. Brevi Note, Istituto Italiano di Preistoria e Protostoria, Padova.

Daily, W., Ramirez, A., 1995. Electrical-resistance tomography during in-situ trichloroethylene remediation at the Savanna River site. J. Appl. Geophys. 33, 239–249.

Daily, W.A., Ramirez, A., Binley, A., LaBrecque, D., 2004. Electrical resistivity tomography. Lead. Edge 23 (5), 438–442.

Daily, W.D., Ramirez, A.L., LaBrecque, D.J., Barber, W., 1995. Electrical resistance tomography experiments at the Oregon Graduate Institute. J. Appl. Geophys. 33, 227–237.

Daily, W., Ramirez, A., LaBrecque, D., Nitao, J., 1992. Electrical resistivity tomography of vadose water movement. Water Resour. Res. 28, 1429–1442.

Day-Lewis, F.D., Lane, J.W., Harris Jr., J.M., Gorelick, S.M., 2003. Time-lapse imaging of saline-tracer transport in fractured rock using difference-attenuation radar tomography. Water Resour. Res. 39, 1290–1303. https://doi.org/10.1029/2002WR001722.

De Carlo, L., Perri, M.T., Caputo, M.C., Deiana, R., Vurro, M., Cassiani, G., 2013. Characterization of the confinement of a dismissed landfill via electrical resistivity tomography and mise-à-la-masse. J. Appl. Geophys. 98 (2013), 1–10. https://doi.org/10.1016/j.jappgeo.2013.07.010.

Deiana, R., Cassiani, G., Kemna, A., Villa, A., Bruno, V., Bagliani, A., 2007. An experiment of non invasive characterization of the vadose zone via water injection and cross-hole time-lapse geophysical monitoring. Near Surf. Geophys. 5, 183–194.

Deiana, R., Cassiani, G., Villa, A., Bagliani, A., Bruno, V., 2008. Model calibration of a water injection test in the vadose zone of the Po River plain using GPR cross-hole data. Vadose Zone J. 7, 215–226. https://doi.org/10.2136/vzj2006.0137.

Deidda, G.P., Balia, R., 2001. An ultrashallow SH-wave seismic reflection experiment on a subsurface ground model. Geophysics 66 (4), 1097–1104.

Deidda, G.P., Diaz de Alba, P., Rodriguez, G., 2017. Identifying the magnetic permeability in multi-frequency EM data inversion. Electron. Trans. Numer. Anal. 47, 1–17. ISSN: 1068-9613.

Deidda, G.P., Fenu, C., Rodriguez, G., 2014. Regularized solution of a nonlinear problem in electromagnetic sounding. Inverse Prob. 30, 1–27. ISSN: 0266-5611. https://doi.org/10.1088/0266-5611/30/12/125014.

Foti, S., Lai, C.G., Rix, G.J., Strobbia, C., 2017. Surface Wave Methods for Near-Surface Site Characterization. CRC Press (9781138077737).

Grote, K., Hubbard, S., Rubin, Y., 2003. Field-scale estimation of volumetric water content using ground-penetrating-radar wave techniques. Water Resour. Res. 39, 1321. https://doi.org/10.1029/2003WR002045.

Haaken, K., Deidda, G.P., Cassiani, G., Deiana, R., Putti, M., Paniconi, C., Scudeler, C., Kemna, A., 2017. Flow dynamics in hyper-saline aquifers: hydro-geophysical monitoring and modeling. Hydrol. Earth Syst. Sci. 21, 1439–1454. ISSN: 1027-5606. https://doi.org/10.5194/hess-21-1439-2017.

Hubbard, S.S., Peterson, J.E., Majer Jr., E.L., Zawislanski, P.T., Williams, K.H., Roberts, J., Wobber, F., 1997. Estimation of permeable pathways and water content using tomographic radar data. Lead. Edge 16, 1623–1628.

Huisman, J.A., Hubbard, S.S., Redman, J.D., Annan, A.P., 2003. Measuring soil water content with ground penetrating radar: a review. Vadose Zone J. 2, 477–491.

Jones, R.B., 1958. In-situ measurement of the dynamic properties of the soil by vibration methods. Geotechnique 8 (1), 1–21.

Jones, R.B., 1962. Surface wave technique for measuring the elastic properties and thickness of roads: theoretical development. Br. J. Appl. Phys. 13, 21–29.

Kästner, M., Braeckvelt, M., Döberl, G., Cassiani, G., Papini, M.P., Leven-Pfister, C., Van Ree, D., 2012. Model-Driven Soil Probing, Site Assessment and Evaluation: Guidance on Technologies. University of Rome La Sapienza Press, Rome, Italy. ISBN: 978-88-95814-72-8.

Keller, G.V., Frischknecht, F.C., 1966. Electrical Methods in Geophysical Prospecting, International Series of Monographs in Electromagnetic Waves. vol. 10. Pergamon Press Inc, Oxford. 525 p.

Kelly, W.E., 1977. Geoelectrical sounding for estimating hydraulic conductivity. Ground Water 15, 420–425.

Kemna, A., Binley, A., Cassiani, G., Niederleithinger, E., Revil, A., Slater, L., Williams, K.H., Flores Orozco, A., Haegel, F.-H., Hördt, A., Kruschwitz, S., Leroux, V., Titov, K., Zimmermann, E., 2012. An overview of the spectral induced polarization method for near-surface applications. Near Surf. Geophys. 10 (6), 453–468. https://doi.org/10.3997/1873-0604.2012027.

Kemna, A., Binley, A., Ramirez, A., Daily, W., 2000. Complex resistivity tomography for environmental applications. Chem. Eng. J. 77, 11–18.

Kemna, A., Binley, A., Slater, L., 2004. Cross-borehole IP imaging for engineering and environmental applications. Geophysics 69, 97–105.

Kemna, A., Vanderborght, J., Kulessa, B., Vereecken, H., 2002. Imaging and characterisation of subsurface solute transport using electrical resistivity tomography (ERT) and equivalent transport models. J. Hydrol. 267, 125–146.

Keskinen, J., Klotzsche, A., Looms, M.C., Moreau, J., van der Kruk, J., Holliger, K., Stemmerik, L., Nielsen, L., 2017. Full-waveform inversion of Crosshole GPR data: implications for porosity estimation in chalk. J. Appl. Geophys. 140, 102–116. https://doi.org/10.1016/j.jappgeo.2017.01.001.

Klenk, P., Jaumann, S., Roth, K., 2015. Quantitative high-resolution observations of soil water dynamics in a complicated architecture using time-lapse ground-penetrating radar. Hydrol. Earth Syst. Sci. 19, 1125–1139. https://doi.org/10.5194/hess-19-1125-2015.

Klotzsche, A., Jonard, F., Looms, M.C., van der Kruk, J., Huisman, J.A., 2018. Measuring soil water content with ground penetrating radar: a decade of progress. Vadose Zone J. 17 (1). https://doi.org/10.2136/vzj2018.03.0052. Article Number: UNSP 180052.

LaBrecque, D.J., Ramirez, A.L., Daily, W.D., Binley, A.M., Schima, S.A., 1996. ERT monitoring of environmental remediation processes. Meas. Sci. Technol. 7, 375–383.

Lesmes, G., Friedman, S., 2005. Relationships between the electrical and hydrogeological properties of rocks and soils. In: Rubin, Y., Hubbard, S.S. (Eds.), Hydrogeophysics. The Netherlands, Springer, Dordrecht, pp. 87–128.

Looms, M.C., Binley, A., Jensen, K.H., Nielsen, L., Hansen, T.M., 2008. Identifying unsaturated hydraulic parameters using an integrated data fusion approach on cross-borehole geophysical data. Vadose Zone J. 7, 238–248.

Manoli, G., Rossi, M., Pasetto, D., Deiana, R., Ferraris, S., Cassiani, G., Putti, M., 2015. An iterative particle filter approach for coupled hydro-geophysical modeling and inversion of a controlled infiltration experiment. J. Comput. Phys. 37–51. https://doi.org/10.1016/j.jcp.2014.11.035.

Mary B., Peruzzo L., Boaga J., Schmutz M., Wu Y., Hubbard S.S. and Cassiani G., Small scale characterization of vine plant root water uptake via 3D electrical resistivity tomography and Mise-à-la-Masse method, Hydrol. Earth Syst. Sci. https://doi.org/10.5194/hess-2018-238.

McMechan, G.A., Yedlin, M.J., 1981. Analysis of dispersive waves by wave field transformation. Geophysics 46, 869874.

Monego, M., Cassiani, G., Deiana, R., Putti, M., Passadore, G., Altissimo, L., 2010. Tracer test in a shallow heterogeneous aquifer monitored via time-lapse surface ERT. Geophysics 75 (4), WA61–WA73. https://doi.org/10.1190/1.3474601.

Nabighian, M.N., Macnae, J.C., 1991. Time domain electromagnetic prospecting methods. In: Nabighian, M.N. (Ed.), Electromagnetic Methods in Applied Geophysics, 02, Society of Exploration Geophysicists. vol. 1991. pp. 427–520.

Naudet, V., Revil, A., Bottero, J.V., Bégassat, P., 2003. Relationship between self-potential (SP) signals and redox conditions in contaminated groundwater. Geophys. Res. Lett. 30, 2091. https://doi.org/10.1029/2003GL018096.

Nazarian, S., Stokoe II, K.H., 1984. In situ shear wave velocity from spectral analysis of surface waves: proceeding of the 8th conference on earthquake. Engineering 3, 31–38.

Ntarlagiannis, D., Williams, K.H., Slater, L., Hubbard, S., 2006. Low-frequency electrical response to microbial induced sulfide precipitation. J. Geophys. Res. 110. https://doi.org/10.1029/2005JG000024.

Park, C.B., Miller, R.D., Xia, J., 1999. Multichannel analysis of surface waves. Geophysics. 64(3).

Parsekian, A.D., Bradford, J., Tsoflias, G., Arcone, S., Kulessa, B., 2016. Advancements in the measurement of the cryosphere using geophysics—introduction. Geophysics 81 (1), WAI–WAII. https://doi.org/10.1190/2015-1120-SPSEINTRO.1.

Perri, M.T., Cassiani, G., Gervasio, I., Deiana, R., Binley, A.M., 2012. A saline tracer test monitored via both surface and cross-borehole electrical resistivity tomography: comparison of time-lapse results. J. Appl. Geophys. 79, 6–16. https://doi.org/10.1016/j.jappgeo.2011.12.011.

Perri, M.T., De Vita, P., Masciale, R., Portoghese, I., Chirico, G.B., Cassiani, G., 2018. Time-lapse Mise-á-la-Masse measurements and modelling for tracer test monitoring in a shallow aquifer. J. Hydrol. 561, 461–477. https://doi.org/10.1016/j.jhydrol.2017.11.013.

Petersen, T., Al Hagrey, S.A., 2009. Mapping root zones of small plants using surface and borehole resistivity tomography. Lead. Edge (10), 1220–1224.

Petronio, L., Boaga, J., Cassiani, G., 2016. Characterization of the Vajont landslide (North-Eastern Italy) by means of reflection and surface wave seismics. J. Appl. Geophys. 128 (2016), 58–67. https://doi.org/10.1016/j.jappgeo.2016.03.012.

Piccolroaz, S., Majone, B., Palmieri, F., Cassiani, G., Bellin, A., 2015. On the use of spatially distributed, time-lapse micro-gravity surveys to inform hydrological modeling. Water Resour. Res. 51 (9), 7270–7288. https://doi.org/10.1002/2015WR016994.

Preti, F., Guastini, E., Penna, D., Dani, A., Cassiani, G., Boaga, J., Deiana, R., Romano, N., Nasta, P., Palladino, M., Errico, A., Giambastiani, Y., Trucchi, P., Tarolli, P., 2018. Conceptualization of water flow pathways in agricultural terraced landscapes. Land Degrad. Dev. 29 (3), 651–662. https://doi.org/10.1002/ldr.2764.

Raffelli, G., Previati, M., Canone, D., Gisolo, D., Bevilacqua, I., Capello, G., Biddoccu, M., Cavallo, E., Deiana, R., Cassiani, G., Ferraris, S., 2017. Local and plot scale measurements of soil moisture: an overview of different techniques applied in plain, hill and mountain experimental sites. Water 9 (9), 706. https://doi.org/10.3390/w9090706.

Robinson, D.A., Binley, A., Crook, N., Day-Lewis, F., Ferré, P.T., Grauch, V.J.S., Knight, R., Knoll, M., Lakshmi, V., Miller, R., Nyquist, J., Pellerin, L., Singha, K., Slater, L., 2007. Advancing process-based watershed hydrological research using near-surface geophysics: a vision for, and review of, electrical and magnetic geophysical methods. Hydrol. Process. 22, 3604–3635.

Robinson, D.A., Lebron, I., Kocar, B., Phan, K., Sampson, M., Crook, N., Fendorf, S., 2009. Time-lapse geophysical imaging of soil moisture dynamics in tropical deltaic soils: an aid to interpreting hydrological and geochemical processes. Water Resour. Res. 45, W00D32. https://doi.org/10.1029/2008WR006984.

Rossi, M., Manoli, G., Pasetto, D., Deiana, R., Ferraris, S., Strobbia, C., Putti, M., Cassiani, G., 2015. Coupled inverse modeling of a controlled irrigation experiment using multiple hydro-geophysical data. Adv. Water Resour. 82, 150–165. https://doi.org/10.1016/j.advwatres.2015.03.008.

Rubin, Y., Hubbard, S.S. (Eds.), 2005. Hydrogeophysics. Springer, Dordrecht, p. 523.

Schlumberger, C., 1920. Étude sur la prospection électrique du sous-sol. Gauthier-Villars, Paris.

Schmalholz, J., Stoffregen, H., Kemna, A., Yaramanci, U., 2004. Imaging of water content distributions inside a lysimeter using GPR tomography. Vadose Zone J. 3, 1106–1115.

Seigel, H.O., 1959. Mathematical formulation and type curves for induced polarization. Geophysics 24 (3), 547–565.

Singha, K., Gorelick, S.M., 2005. Saline tracer visualized with three-dimensional electrical resistivity tomography: field-scale spatial moment analysis. Water Resour. Res. 41.

Slater, L., Binley, A., Brown, D., 1997. Electrical imaging of fractures using ground-water salinity change. Groundwater 35, 436–442.

Slater, L., Binley, A.M., Daily, W., Johnson, R., 2000. Cross-hole electrical imaging of a controlled saline tracer injection. J. Appl. Geophys. 44, 85–102.

Strobbia, C., Cassiani, G., 2007. Multi layer GPR guided waves in shallow soil layers for the estimation of soil water content. Geophysics 72, 17–29. https://doi.org/10.1190/1.2716374.

Strobbia, C., Foti, S., 2006. Multi-offset phase analysis of surface wave data (mopa). J. Appl. Geophys. 59, 300–313.

Sumner, J.S., 1976. Principles of Induced Polarisation for Geophysical Exploration. Elsevier, Amsterdam.

Telford, W.M., Geldart, L.P., Sheriff, R.E., 1990. Applied Geophysics, Second ed. Cambridge University Press, pp. 645–700.

Topp, G.C., Davis, J.L., Annan, A.P., 1980. Electromagnetic determina¬tion of soil water content: measurements in coaxial transmission lines. Water Resour. Res. 16, 574–582.

van Overmeeren, R.A., Sariowan, S.V., Gehrels, J.C., 1997. Ground penetrating radar for determining volumetric soil water content: results of comparative measurements at two test sites. J. Hydrol. 197, 316–338.

Vanella, D., Cassiani, G., Busato, L., Boaga, J., Barbagallo, S., Binley, A., Consoli, S., 2018. Use of small scale electrical resistivity tomography to identify soil-root interactions during deficit irrigation. J. Hydrol. 556, 310–324. https://doi.org/10.1016/j.jhydrol.2017.11.025.

Vereecken, H., Binley, A., Cassiani, G., Kharkhordin, I., Revil, A., Titov, K. (Eds.), 2006. Applied Hydrogeophysics. Springer-Verlag, Berlin, p. 372.

Viezzoli, A., Christiansen, A.V., Auken, E., Sørensen, K., 2008. Quasi-3d modeling of airborne tem data by spatially constrained inversion. Geophysics 73, F105–F113. https://doi.org/10.1190/1.2895521.

Vignoli, G., Cassiani, G., 2010. Identification of lateral discontinuities via multi-offset phase analysis of surface wave data. Geophys. Prospect. 58, 389413.

Vignoli, G., Cassiani, G., Rossi, M., Deiana, R., Boaga, J., Fabbri, P., 2012. Geophysical characterization of a small pre-alpine catchment. J. Appl. Geophys. 80, 32–42. https://doi.org/10.1016/j.jappgeo.2012.01.007.

Vignoli, G., Gervasio, I., Brancatelli, G., Boaga, J., Della Vedova, B., Cassiani, G., 2016. Frequency-dependent multi-offset phase analysis of surface waves: an example of high resolution characterization of a riparian aquifer. Geophys. Prospect. 64 (1), 102–111. https://doi.org/10.1111/1365-2478.12256.

Vignoli, G., Strobbia, C., Cassiani, G., Vermeer, P., 2011. Statistical multi-offset phase analysis (sMOPA) for surface wave processing in laterally varying media. Geophysics 76, U1–U11. https://doi.org/10.1190/1.3542076.

von Hebel, C., Matveeva, M., Verweij, E., Rademske, P., Kaufmann, M.S., Brogi, C., Vereecken, H., Rascher, U., van der Kruk, J., 2018. Understanding soil and plant interaction by combining ground-based quantitative electromagnetic induction and airborne Hyperspectral data. Geophys. Res. Lett. 45 (15), 7571–7579. https://doi.org/10.1029/2018GL07865.

Weill, S., Altissimo, M., Cassiani, G., Deiana, R., Marani, M., Putti, M., 2013. Saturated area dynamics and streamflow generation from coupled surface–subsurface simulations and field observations. Adv. Water Resour. 59, 196–208. https://doi.org/10.1016/j.advwatres.2013.06.007.

Yilmaz, Ö., 2001. Seismic Data Analysis. Society of Exploration Geophysicists. ISBN: 1-56080-094-1.

Zhang, J., Brink, U.S., Toksöz, M.N., 1998. Nonlinear refraction and reflection travel time tomography. J. Geophys. Res. 103 (B12), 29743–29757.

Zonge, K.L., Hughes, L.J., 1991. In: Nabighian, M.N. (Ed.), Controlled Source Audio-Frequency Magnetotellurics, Electromagnetic Methods in Applied Geophysics. Vol. 2, Society of Exploration Geophysicists, pp. 713–809.

Further reading

Binley, A.M., 2018. Profiler/R2t Codes. www.es.lancs.ac.uk/people/amb/Freeware.

Brovelli, A., Cassiani, G., 2011. Combined estimation of effective electrical conductivity and permittivity for soil monitoring. Water Resour. Res.. 47. https://doi.org/10.1029/2011WR010487.